

## Ultrasound-responsive Nanocarriers in Cancer Treatment- a review

Received 00th January 20xx,  
Accepted 00th January 20xx

DOI: 10.1039/x0xx00000x

**Nahid S. Awad<sup>a</sup>, Vinod Paul<sup>a</sup>, Nour Alsawafth<sup>a</sup>, Gail ter Haar<sup>b</sup>, Theresa M. Allen<sup>c</sup>, William G. Pitt<sup>d</sup> and Ghaleb A. Hussein<sup>\*a</sup>**

**Abstract:** The safe and effective delivery of anticancer agents to diseased tissues is one of the significant challenges in cancer therapy. Conventional anticancer agents are generally cytotoxins with poor pharmacokinetics and bioavailability. Nanocarriers are nanosized particles, a few of which have received clinical approval, which increase the selectivity of anti-cancer drugs and genes transport to tumors. They are small enough to extravasate into solid tumors where they slowly release their therapeutic load by passive leakage or by biodegradation. Using smart nanocarriers, the rate of release of the entrapped therapeutic(s) can be increased, and greater exposure of the tumor cells to the therapeutics can be achieved when the nanocarriers are exposed to certain internally (enzymes, pH and temperature) or externally applied (light, magnetic field, and ultrasound) stimuli that trigger the release of their load in a safe and controlled manner, spatially and temporally. This review gives a comprehensive overview of recent research findings on the different types of stimuli-responsive nanocarriers and their application in cancer treatment, with a particular focus on ultrasound.

**Keywords:** Nanocarriers, Chemotherapy, Ultrasound, drug release.

### 1. INTRODUCTION

Cancer is the second leading cause of global mortality, with 17 million new cases reported in 2018, and 9.6 million reported deaths in the same year.<sup>1</sup> Given the high incidence of morbidity and mortality, it is essential that more research is directed towards developing more effective methods of prevention, early detection, and treatment of the disease. Despite advances in molecular cancer therapeutics, traditional cancer therapies, such as small molecule chemotherapy, are still widely used to suppress cancer cell proliferation, in efforts to control its progression and metastasis. Many of the small molecule therapeutics used in conventional chemotherapy have poor aqueous solubility resulting in a large volume of distribution throughout the body, causing toxic side effects to normal tissues, while only a very small percentage reaches diseased tissue.<sup>2</sup> These agents, therefore, have a low therapeutic index with a narrow window of concentration between toxicity and therapeutic effect. Raising the dose to achieve an increased therapeutic effect also increases the levels of dose-limiting adverse effects. Since chemotherapeutics have poor selectivity, i.e., poor ability to differentiate between malignant and benign cells (which have high division rates such as those in the bone marrow, hair follicles, digestive tract, and reproductive system) they kill both healthy and cancerous cells. This lack of selectivity results in a number of toxic side effects including nausea, vomiting, fatigue, hair loss, anemia, diarrhea, cardiac problems and sexual dysfunction.

The pathophysiology of some tumors creates a bed of abnormal, highly permeable capillaries that bring oxygen and nutrients to the tumor cells. Nano-sized carriers (nanocarriers), encapsulating anti-neoplastic agents, are small enough to extravasate from the vasculature into the interstitial space surrounding the tumor cells, increasing the delivery of their cargo to the tumor site. Encapsulation significantly reduces the delivery of cytotoxic drugs to healthy tissues, which have normal, poorly permeable vessels. Nanocarriers also improve the solubility of some drugs, prolong their therapeutic lifetime, and increase their therapeutic benefit.<sup>3</sup> Hence, encapsulation of anticancer therapeutics in nanocarriers maintains or improves the efficacy of the treatment, while reducing the side effects to healthy tissues. Some receptors are overexpressed on the surfaces of the tumor cells, and these molecules can be targeted with nanocarriers decorated with targeting moieties complementary to the overexpressed receptors.<sup>4</sup>

As shown in Figure 1, nanocarriers that are designed to encapsulate drug molecules within a membrane are referred to as “nanocapsules”, while other nanocarriers in which the drug molecules are embedded and distributed within a polymer matrix are called “nanospheres”.<sup>5</sup> All types of nanocarriers must encapsulate drugs efficiently and, while the particles are still circulating in the bloodstream, retain the agents without significant release in order to prevent their uptake by healthy tissues. However, upon reaching their desired site of action, these nanocarriers are expected to release their load in an active form.

<sup>a</sup> Department of Chemical Engineering, American University of Sharjah, Sharjah, UAE.

<sup>b</sup> The Institute of Cancer Research, F, Middleton M, Gleeson Sutton, Surrey, UK.

<sup>c</sup> Department of Biochemistry and Molecular Biology, University of British Columbia, Vancouver, Canada

<sup>d</sup> Chemical Engineering Department, Brigham Young University, Provo, USA.

Address correspondence to this author at the Department of Chemical Engineering, Faculty of Engineering, American University of Sharjah, P.O. Box: 26666, Sharjah,

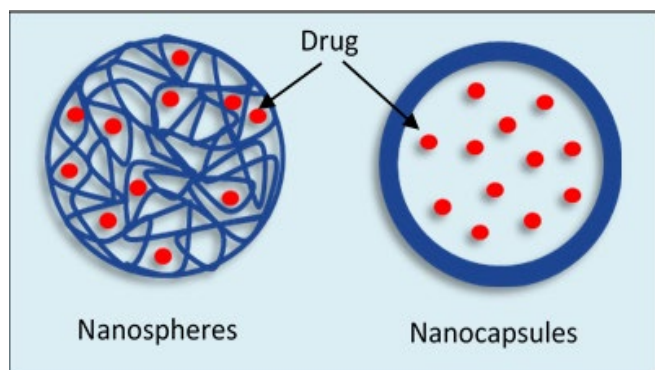


Fig. (1). Schematic representation of nanocarriers encapsulating drugs.

Following their accumulation in tumor tissues, several internal or external stimuli can be employed to trigger drug release from stimuli-responsive nanocarriers (called smart nanocarriers), ensuring a faster and more controllable rate of drug release at the target site. Several release triggers have been investigated. These include light,

at desired locations, while significantly lowering toxic effects in healthy cells.<sup>11</sup>

## 2. NANOCARRIERS USED IN DRUG DELIVERY

A pressing need to improve the pharmacokinetics, biodistribution and therapeutic efficacy of anticancer drugs led to the development (and several subsequent clinical approvals) of a wide range of nanocarriers ranging in size from  $\sim 10$  to 1000 nm. The size of these nanocarriers plays a crucial role in their *in vivo* biodistribution. While particles that are smaller than 5 nm are cleared from the blood rapidly,<sup>12,13</sup> particles larger than 220 nm usually accumulate in the liver, spleen, and bone marrow.<sup>14</sup> Most products in the clinic have sizes of  $\sim 60 - 200$  nm.<sup>15</sup>

Long circulation half-lives are an important attribute, and nanocarriers must evade clearance by biological mechanisms such as the mononuclear phagocytosis. Other important attributes are (1) biocompatibility and safety, (2) efficient drug loading, (3) efficient delivery of the drug to targeted locations in the body, and (4) lack of immunogenicity.<sup>16</sup> The field of nanocarriers has been growing steadily over the past two decades. Several nanoparticles, ranging in size, shape, composition, and physical properties, have been used to

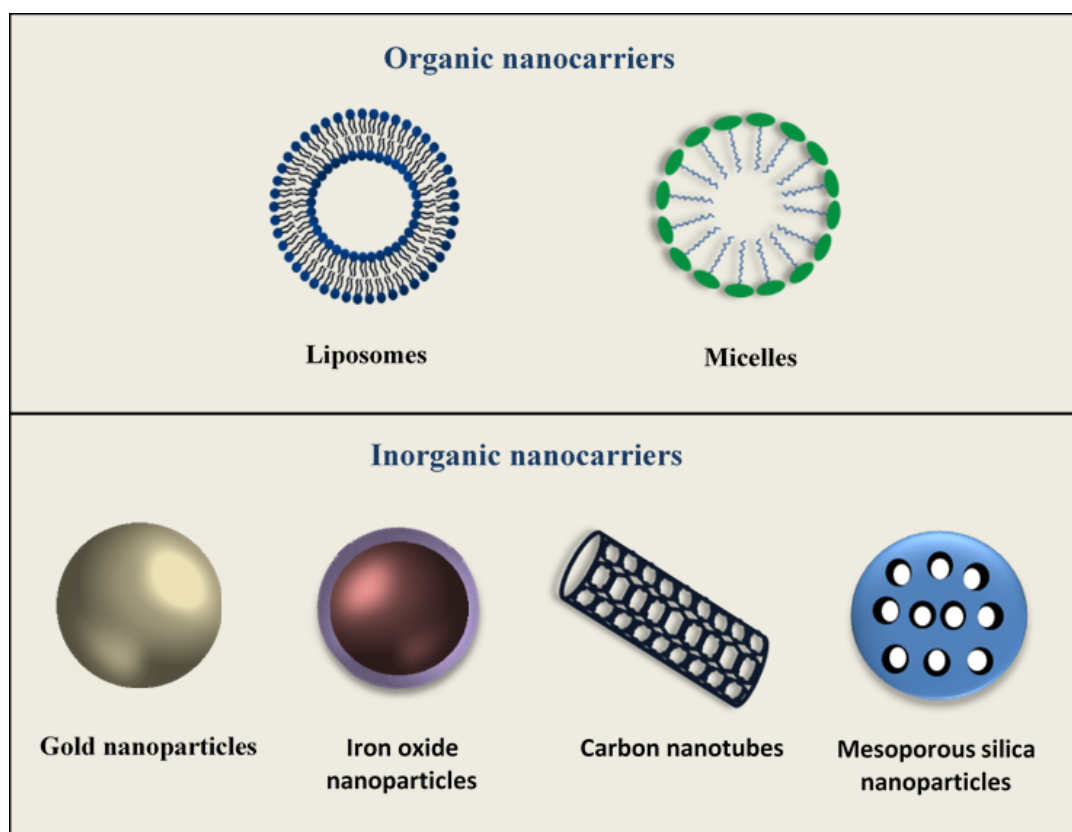


Fig. (2). Organic and inorganic nanocarriers used in drug delivery.

temperature, enzymes, and pH.<sup>6-9</sup> Ultrasound has been shown to be an effective technique for triggering drug release from nanocarriers.<sup>10</sup> Hence, controlled drug delivery systems with associated triggered release mechanisms can increase drug delivery

treat tumors and infections.<sup>17</sup>

Nanocarriers may be organic in nature (such as micelles, liposomes, and dendrimers), or composed of inorganic materials such as mesoporous silica nanoparticles, superparamagnetic iron oxide nanoparticles, carbon nanotubes, gold nanoparticles, metal-organic

frameworks, and quantum dots.<sup>18</sup> Figure 2 shows several nanocarriers, which will be discussed below. The most successful clinical products to date have been lipidic nanoparticles, such as liposomes.

### 2.1. Passive targeting of cancer cells by nanocarriers

Nanocarriers have multiple applications in the field of drug delivery, most particularly in the treatment of cancer, inflammation, and infection. The potential of these nanocarriers in cancer treatment is associated with their passive (or non-selective) targeting of solid tumors, via the “enhanced permeability and retention” (EPR) effect. This occurs when tumors develop new vasculature, during the angiogenesis that supplies their high requirement for oxygen and nutrients. The newly formed capillary endothelium in tumor tissues is disorganized and leaky, with imperfect endothelial cell coverage and improper lymphatic drainage.<sup>19</sup> This leads to the aberrant molecular and fluid dynamic behavior in the tumor. The small size of nanoparticles allows them to extravasate through the leaky vasculature and to accumulate at the diseased site (Figure 3) if circulation half-life is sufficiently long.

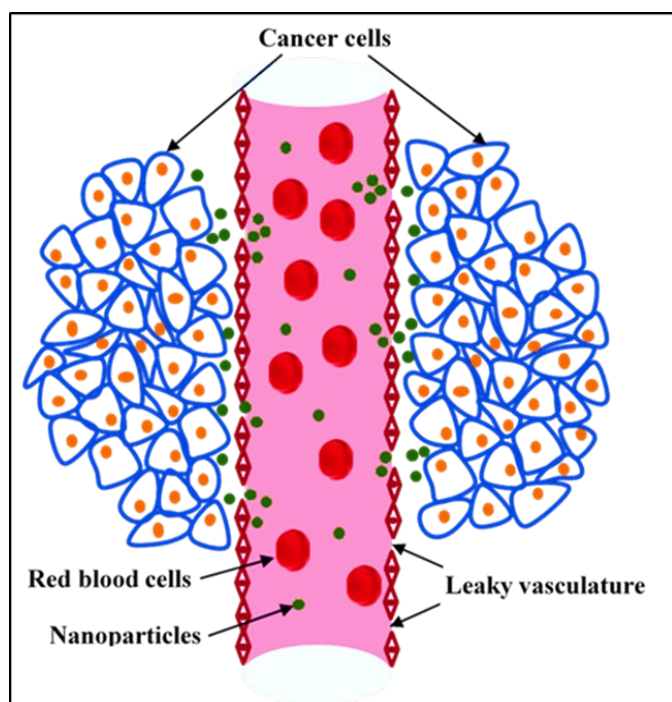


Fig. (3). The leaky blood vessels surrounding the tumor with retarded lymphatic drainage (EPR effect) allows nanoparticles to extravagate through the blood vessels and accumulate inside the tumor.

A commonly used technique to increase their blood circulation times is to graft polymers such as polyethylene glycol (PEG) chains to the particle surface, thus enabling them to reach the tumor circulation and extravasate into the interstitial space at increased concentrations<sup>20</sup> (where there are sufficient angiogenic blood vessels). Some tumors show inherent low drug accumulation by the EPR effect, in others, vessel permeability can be highly heterogeneous.<sup>21</sup>

PEG is non-ionic and highly soluble in water and organic solvents. Conventional liposomes, i.e., those not grafted with PEG or similar polymers, interact with specific proteins (i.e., opsonins) in the bloodstream (a process referred to as opsonization), resulting in their rapid removal from the blood by hepatic and splenic macrophages. However, even with PEGylated particles (so-called ‘stealth’ liposomes), the distribution of the particles to the disease site via the bloodstream (i.e. ‘passive’ targeting) does not ensure the uptake of nanoparticles by the cancer cells. Therapeutics released from the nanoparticles in the vicinity of the tumor cells, e.g., by diffusion across the nanoparticle membrane, can be taken up by normal uptake mechanisms. Hence, there is room for improvements over passive targeting mechanisms.

### 2.2. Ligand-mediated targeting of cancer cells by nanocarriers and triggered release

Tumor-targeting ligands have been used to significantly increase the uptake of nanocarriers into cancer cells. This is accomplished by conjugating targeting moieties that bind to cancer-selective surface ligands to the nanoparticle surface. Ligand-targeted nanocarriers are designed to bind to overexpressed receptors, and to trigger the internalization of the targeted nanocarriers into the cell. Molecules such as proteins, hormones, antibodies, peptides, aptamers, and oligonucleotides are already used to target different types of cancer.<sup>22</sup> The targeted nanocarriers are designed to sequester their drug contents until the carrier and its drug load are delivered to the target site. At that point, a burst release of the payload, triggered by an external stimulus, rather than a slow release of drugs from the nanoparticles by passive diffusion, is the most effective mechanism for achieving a higher drug concentration inside a tumor cell.<sup>23</sup> The triggering mechanism can change a nanocarrier from one with a low release rate to one in an unstable state with a high rate of drug release. This drug release trigger can be achieved by employing the unique characteristics of the tumor’s microenvironment.

Intrinsic components of responsive targeted drug delivery include overexpressed tumor enzymes,<sup>24</sup> low tumor pH,<sup>25</sup> and temperature<sup>26</sup> differences between the tumor and healthy tissues. Nanocarriers can also be designed to be responsive to “external stimuli” such as light,<sup>27</sup> magnetic fields,<sup>28</sup> and ultrasound.<sup>29</sup> Figure 4 shows the three main components of nanocarrier-based targeted drug delivery.

## 3. GENERAL ASPECTS OF ULTRASOUND

Ultrasound consists of pressure waves with a frequency above the audible range for humans, usually defined as being above 20 kHz. Ultrasound can be further classified into low-frequency ultrasound (frequencies lower than 1 MHz), medium-frequency ultrasound (1–5 MHz), and high-frequency ultrasound (frequencies higher than 5 MHz).<sup>30</sup> Ultrasonic waves propagate in soft tissue as mechanical longitudinal waves, causing alternating regions of compression and rarefaction in the medium. These oscillations in density and pressure can cause several biological effects, which are discussed below.

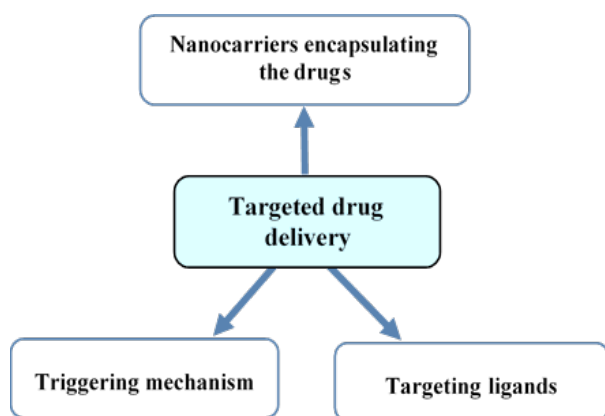


Fig. (4). The key components of responsive targeted nanocarriers drug delivery.

Ultrasound technology has been widely used in the medical field for both diagnostic and therapeutic purposes due to its cost-effectiveness, safety, non-invasiveness, and simplicity. For diagnostic applications, ultrasound parameters such as frequency and intensity are chosen in such a way that they produce minimal biological effects while allowing the production of images with good spatial and temporal resolution. However, for therapeutic applications, reversible or irreversible biophysical effects are often sought.<sup>31</sup> Although there are many therapeutic applications of ultrasound, this review will focus on the applications of ultrasound in cancer treatment. Two ultrasound parameters, that are often manipulated to induce desired biological effects, are the acoustic frequency and intensity. Decreasing acoustic frequency increases the depth of penetration and the likelihood of cavitation, while increasing the intensity may control the amount of energy that can reach a target site. Other factors, such as the exposure time and pulsing regime (i.e., duty cycle) can also be adjusted to create several useful biological effects.

**Frequency.** Ultrasound frequencies used in the medical field vary, depending on the required application. For diagnostic applications, the frequency defines the spatial resolution (i.e., increased resolution is obtained at higher frequencies). However, the penetration depth is reduced, and heating is increased with increasing frequencies. Ultrasound attenuation and absorption by the medium is strongly dependent on frequency.<sup>32</sup> At higher frequencies, ultrasonic energy is more readily absorbed and attenuated, reducing penetration into the deep tissues.

The velocity at which the sound wave propagates in the medium ( $c$ ) is a function of the medium's elasticity ( $K$ ) and density ( $\rho$ ):

$$c = \sqrt{(K/\rho)} \quad (1)$$

The velocity, frequency ( $f$ ) and the wavelength ( $\lambda$ ) are related by

$$c = f\lambda \quad (2)$$

**Acoustic intensity.** As ultrasound waves propagate, regions of high pressure (compression) and low pressure (rarefaction) move through

the medium. The amplitude of an ultrasonic wave can be defined as the difference between peak compression and rarefaction values, ( $p^+ + p^-$ ). The pressure wave causes physical displacement of molecules, with an amplitude of  $P^+/( \rho c)$ , where  $P^+$  is the peak compression pressure. Ultrasound intensity ( $I$ ), which is a function of pressure, is defined as the amount of power produced by the ultrasound wave divided by the surface area through which it propagates. " $I$ " is measured in  $W/cm^2$ , and is directly related to the acoustic pressure ( $P$ ), the density of the medium ( $\rho$ ) and the ultrasound propagation velocity in the medium ( $c$ ) by:

$$I = \frac{P^2}{\rho c} \quad (3)$$

When ultrasound passes through the tissues, it induces mechanical, thermal, and sometimes chemical effects. All these effects have the potential for use in cancer treatment applications.

### 3.1. Mechanical effects of ultrasound

The two main mechanisms that cause mechanical effects are cavitation and ultrasound radiation force.

#### 3.1.1. Cavitation

Cavities or bubbles either pre-exist in the liquid or are created due to the pressure drop to a value lower than the vapor pressure of the liquid. The formation, oscillation, growth, and collapse of these cavities in an ultrasonic field is called acoustic cavitation. The behavior of the cavitation bubbles varies depending on the pressure, frequency, the radius of the bubbles, and the physical properties of the surrounding fluid (e.g., viscosity, and compressibility). The probability of cavitation occurrence increases as the pressure increases and generally decreases with frequency. Depending upon the behavior of the bubble, oscillations can be classified as stable (non-inertial) cavitation or inertial cavitation (also called transient or collapse cavitation).

Stable cavitation occurs when the acoustic pressure is at a level for which bubble response is generally linear. The bubbles oscillate around an equilibrium radius value in each acoustic cycle (Figure 5). This oscillation results in microstreaming in the surrounding fluid, fluid shear stresses, and localized generation of heat.<sup>33,34</sup> During the negative pressure phase, dissolved gas diffuses into the bubbles and continues to accumulate inside these bubbles leading to an increase in size, with the opposite occurring during the positive pressure portion of the cycle, but to a lesser extent. With continued exposure, the bubbles grow in size with the net transport of gas into these bubbles.

Inertial or collapse cavitation occurs at higher peak negative pressures or when the bubble size grows to its natural resonance size, leading to large amplitude oscillations. Under these conditions, the bubbles oscillate non-linearly, producing subharmonic and higher (ultra-) harmonic oscillations. During the positive pressure phase, the compression by the inward-moving surrounding liquid collapses the gas bubble to the point of a supercritical fluid, creating

pressures exceeding 100 atm (Figure 5). This collapse generates shock waves of very high pressures and produces high local temperatures. If the collapse is not symmetrical, high-speed liquid microjets are generated at the microscopic level.<sup>33,35–37</sup> Cavitation can produce not only mechanical effects but also thermal and chemical effects in adjacent tissues. These physicochemical effects will be discussed below. The Mechanical Index (MI) describes the possibility of the occurrence of cavitation. To avoid tissue damage during diagnostic imaging, the U.S. Food and Drug Administration (FDA) restricts the MI to less than 1.9. The MI is calculated as  $MI = P^- / \sqrt{f}$ , where  $P^-$  is the peak negative pressure in MPa, and  $f$  is the central frequency of the ultrasound wave in MHz.

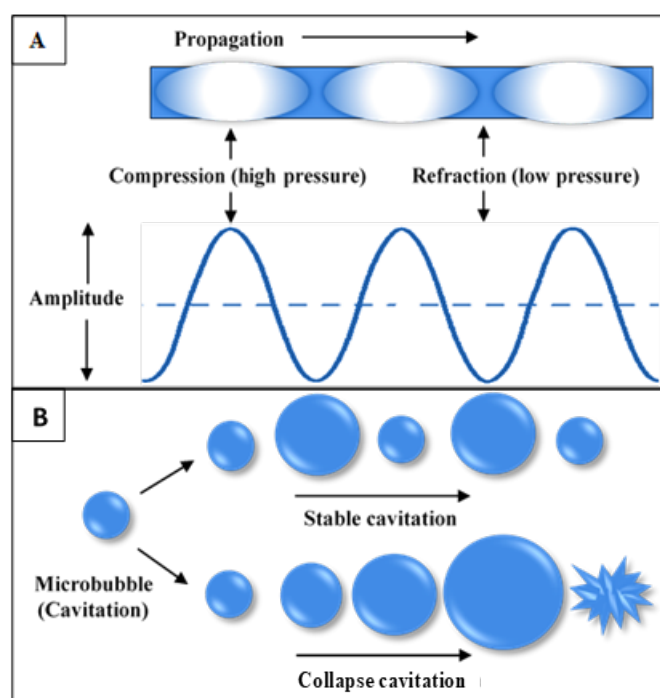


Fig. (5). Schematic representation of the acoustic pressure waves (A), stable and collapsed cavitation of microbubbles (B).

### 3.1.1.1. Sonoporation

Sonoporation is the process of pore formation in a cell membrane upon exposure to ultrasound. It is a cavitation induced biological effect that is often leveraged for drug delivery. From a therapeutic point of view, sonoporation enables membrane-impermeable compounds to enter the cells through defects generated in the cell membrane. Sonoporation occurs as a result of several mechanisms. Firstly, asymmetric inertial cavitation can produce high-speed microjets that pierce the cell membrane. This asymmetry can occur when the cavitating bubble is near a cell surface.<sup>38</sup> Stable cavitation or inertial cavitation can generate a local steady or transient 'microstreaming' flow that produces holes by shearing<sup>39</sup> or stretching the cell membrane.<sup>40</sup> Wu et al.<sup>41</sup> have shown that by using a mason horn at 21 kHz, shear stress of over 12 Pa on the cell membrane can cause sonoporation. Some of their theoretical analysis has shown that 92 Pa shear stress can be generated by the

microstreaming caused by ultrasound at 2 MHz and 0.1 MPa. As the acoustic pressure increased to 0.4 MPa, the shear stress also increased to 1100 Pa.<sup>40</sup> As illustrated in Figure (6), the compression and expansion of the bubble near the cell membrane can cause membrane disruption. In addition, the radiation forces produced by the ultrasound waves may push the bubble towards the cell membrane, eventually disrupting its integrity.<sup>42</sup> Increasing the amplitude of ultrasound leads to a rapid increase in the oscillation amplitude of the bubble. The collapse of the bubble creates shock waves and microjets if the collapse is near to a surface such as a vessel wall, leading to an increase in the size and number of pores created on the cell membrane. Ultrasound parameters have a direct effect on the pore size.<sup>43</sup> Transient pore sizes of up to 4  $\mu\text{m}$  were created in the membrane of MCF-7 breast cancer cells when exposed to moderate ultrasound (0.25 MPa) assisted by the addition of encapsulated 1- $\mu\text{m}$  diameter microbubbles.<sup>44</sup>

### 3.1.1.2 Free Radical Formation

During inertial cavitation, extremely high temperatures (above 5000 K) and pressures (above 1000 atm) are produced. This leads to the thermal dissociation of the water and, therefore, the formation of hydrogen atoms and hydroxyl radicals.<sup>45</sup> Sonosensitive nanoparticles are often added to create free radicals, which enhances effects such as sonoluminescence and pyrolysis.<sup>46</sup> Light emission ensues immediately following the collapse of the bubbles when the excited chemical species are relaxed, or radicals recombine; the emitted light can then activate certain sensitizers. These sensitizers produce an electron-hole ( $e^-/h^+$ ) pair leading to the production of reactive oxygen species (ROS) in an aqueous environment.<sup>47</sup> In pyrolysis, the high temperature generated by the collapse of the cavity chemically excites the sensitizer, producing highly reactive free radicals that form ROS when reacting with other molecules in the aqueous environment.<sup>48</sup>

The most common sonochemical effects are mainly produced by two ROS: hydroxyl free radicals and singlet molecular oxygen. The production of ROS will depend on the sonosensitizer used, the intensity of ultrasound, and the frequency and strength of the cavitation events. The reactive hydroxyl free radicals are formed by the pyrolysis of water occurring as a result of a collapse event. These free radicals can further react with nearby water to produce hydroperoxide radicals or can react with non-volatile solutes such as DNA and modify its purine and pyrimidine bases.<sup>49,50</sup> When reactive oxygen species are not adequately removed from the medium, oxidative stresses on the cells result in severe metabolic dysfunction, including peroxidation of membrane lipids, cytoskeletal disruption, generation of protein radicals, modification to nucleic acids, DNA damage, and cell death.<sup>50,51</sup> The formation of free radicals can happen either in extracellular or intracellular spaces. Those formed outside the cells are short-lived, and their bioeffects are doubtful unless they react with the solutes and produce toxic compounds.<sup>52</sup>

### 3.1.1.3 Endocytosis

Macromolecules larger than 1 kDa cannot penetrate the external lipid bilayer structure of the cell membranes. The cell possesses a variety of internalization mechanisms, collectively called endocytosis, to internalize these complex molecules. Endocytosis can occur through different mechanisms that can be mediated by, for example, clathrin or caveolae. Although the usual explanation for ultrasound-assisted drug uptake is sonoporation, there is evidence that specific physicochemical stimuli such as mechanical forces or free radicals can promote the internalization of molecules into cells by various endocytic mechanisms. For example, the shear stress

GST-Tatt11-EFGP and exposed to ultrasound at a mechanical index of 1.2 for 30 minutes showed increased internalization of the compound over that seen in the control sample with no alterations in cell viability and membrane integrity. Adding free radical generation inhibitors reduced the cellular internalization by 50 %, indicating that endocytosis is partially mediated by ROS formation. Another study by Tardoski et al.<sup>57</sup> showed that low-intensity ultrasound promoted clathrin-mediated endocytosis. It was also demonstrated that following sonication, the transport mechanism of macromolecules happens either through transient pores or through

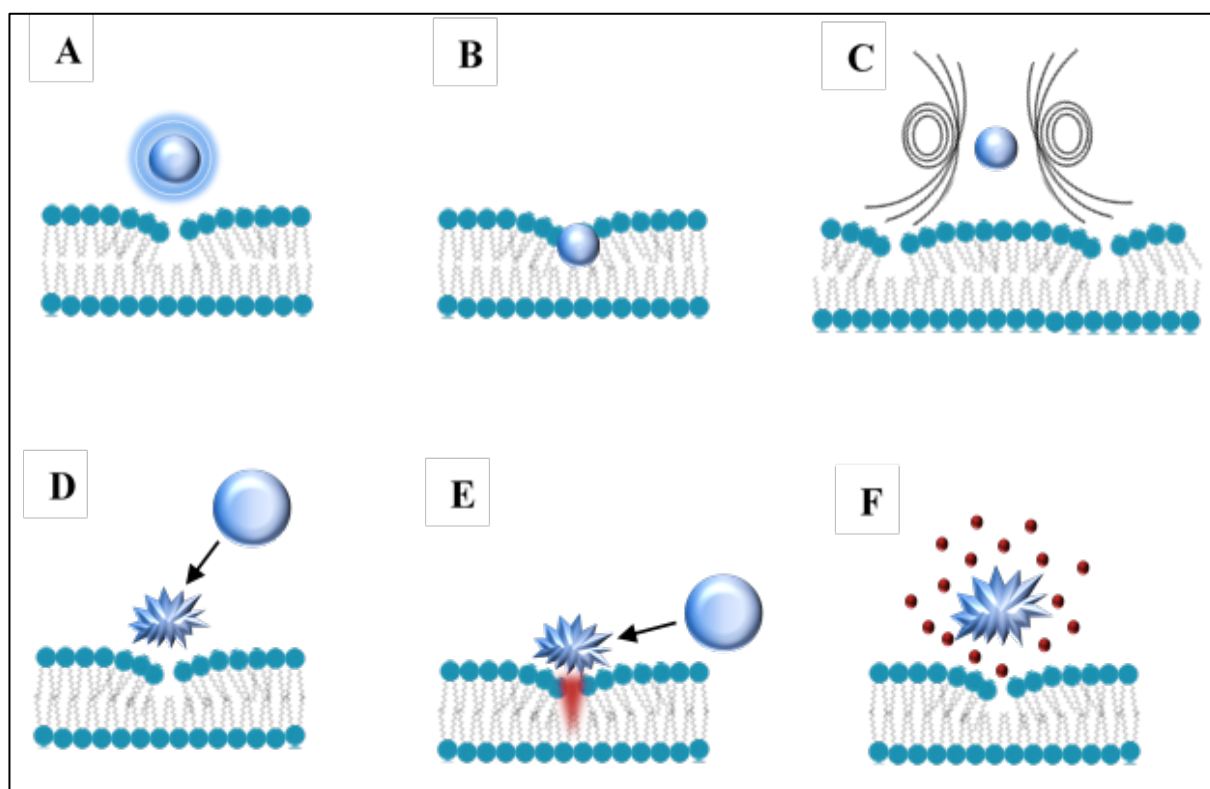


Fig. (6). Different mechanisms by which oscillating microbubbles may disrupt the integrity of cell membranes. A: Stable cavitation produces shear forces that can perturb membrane structure. B: Stable cavitation generates radiation forces that push microbubbles towards the cell and possibly through the cell membrane. C: The mechanical stress created by microstreaming around microbubbles during stable cavitation, causes pore formation. D: During inertial cavitation, the shock waves formed by the collapsing microbubbles generate high pressure which disrupts the cell membrane. E: The asymmetrical collapse of microbubble accelerates a microjet toward the cell membrane, forming a pore. F: During inertial cavitation, reactive oxygen species (ROS) can be formed. This leads to the disruption of the cell membrane through lipid peroxidation.

created by ultrasound on the cell membranes has been found to induce endocytosis.<sup>39</sup> Both sonoporation and endocytosis were involved in enhancing the uptake of nanocarriers by the cells following sonication.<sup>53,54</sup> Mechanical sensors such as integrins and ion channels sense the mechanical deformation of the cytoskeleton by ultrasound and can convert these signals to activate endocytosis.<sup>55</sup>

Lionetti et al.<sup>56</sup> reported that the application of diagnostic ultrasound (1.6 MHz and 1.2 MI) for 30 mins *in vitro* enhanced caveolae-mediated endocytosis. The study reported that cells treated with

endocytosis, depending on the molecular size.<sup>58</sup>

### 3.1.2. Acoustic radiation forces

Acoustic radiation forces are exerted by ultrasound on an object in the acoustic field. It may cause biological effects. This force is given by  $W/c$ , where  $W$  is the acoustic power, and  $c$  is the speed of sound traveling through the medium. When ultrasound propagates through a medium, absorption of wave energy imparts kinetic energy to the fluid, leading to localized fluid flow, a phenomenon known as acoustic streaming. The flow's velocity ( $v$ ) is given by:

$$v = \frac{2\alpha W}{\mu \rho c} \quad (4)$$

where  $\mu$  is the fluid viscosity, and  $\alpha$  is the absorption coefficient.<sup>32</sup> The beam geometry and kinematic turbulence also influence the streaming velocity.<sup>33</sup>

The radiation force, in the case of complete wave reflection, is:

$$F = 2 \frac{W}{c} \quad (5)$$

These radiation forces, or the acoustic flow they create, can lead to the displacement of the bubbles and particles in the blood, driving particles into the target tissue, and hence creating reversible structural deformations (Figure 6B).<sup>59,60</sup>

### 3.2. Thermal Effects of Ultrasound

In addition to mechanical effects, thermal effects are important by-products of acoustic waves. When pressure waves propagate through tissue, they are attenuated due to absorption and scattering. For a sinusoidal ultrasound wave with frequency  $f$ , and initial pressure amplitude  $P_0$ , the pressure amplitude at point  $x$  from the initial point is given by:

$$P_x = P_0 \exp(-\alpha x) \quad (5)$$

When the acoustic energy is absorbed, it is converted to thermal energy. The amount of energy absorbed by the tissue depends on the absorption coefficient  $\alpha$ , which is frequency-dependent with the relationship shown in the equation below:

$$\alpha = \alpha_0 f^n \quad (6)$$

where  $\alpha_0$  is the reference absorption coefficient of the particular tissue, and  $n$  is a fitted constant. Thus, as ultrasound frequency increases, more of the ultrasound energy will be absorbed by the tissues, producing more heat. Where the temperature-induced is sufficiently high, local ultrasonic mediated heat deposition (hyperthermia) has been shown to kill cells and damage proteins and other cellular structures, while minimizing the adverse effects on adjacent healthy tissues.<sup>60,61</sup>

Raised temperatures have been found to induce apoptotic and necrotic cell death.<sup>60</sup> The main factors that determine the type of hyperthermia-induced cell death are the type of cell, the increase in temperature, and the time for which it is maintained.<sup>62</sup> As the temperature is raised above 43 °C (hyperthermia), changes start to occur, which affect different cellular compartments such as membrane fluidity, thus impeding the function of transmembrane transport protein and receptors located at the cell surface.<sup>63</sup> Cell shape and cytoskeleton changes were observed following heat treatment. Depending on the cell type, cells have been flattened or rounded, while blebbing has also been observed on some cell surfaces.<sup>64–66</sup> Reduction in the expression of membrane proteins and

integrins has also been observed,<sup>67</sup> in addition to protein denaturation.<sup>68</sup>

## 4. ULTRASOUND AND THERAPY

Ultrasound has revolutionized both medical diagnosis and treatment. It has also been used to stimulate and accelerate the healing of bone fractures as well as other injuries to soft tissues.<sup>69</sup> It is also currently used in bone growth stimulation.<sup>31</sup> Diagnostic ultrasound is generally safe and has good tissue penetration with low operational and instrumental costs.<sup>70</sup> As mentioned, several factors control the biological effects of ultrasound: the intensity and frequency of the acoustic waves, the exposure time, and the number of pulses.<sup>71</sup> High intensity focused ultrasound (HIFU) focuses high acoustic energy on a specific focal target, and has been used in cancer treatment. This energy is absorbed by the tissues located at the focal point of treatment, producing an extreme rise in temperature (above 80°C) while not creating cytotoxic temperatures outside the focal zone.<sup>72,73</sup> This results in the total destruction of the targeted cancer cells. HIFU ablation works through the placement of small lesions side by side on the tumor tissues, which requires precision if an entire tumor is to be ablated efficiently.<sup>74</sup> While the thermal effect of HIFU is the main contributor to cancer treatment, non-thermal effects due to acoustic cavitation, such as microstreaming and radiation forces that cause membrane destruction and cell death, are also produced.

HIFU treatment of tumors has been associated with some complications, including second and third-degree skin burns. Additionally, there has been concerns that the rupture of the tumor cells and their surrounding blood vessels may cause metastasis through the bloodstream, although this has not been proven conclusively.<sup>75</sup> The release of inflammatory cytokines may help to stimulate the immune response.<sup>76</sup>

Ultrasound is a major component of a promising cancer treatment known as sonodynamic therapy (SDT). SDT uses low-intensity ultrasound combined with sonosensitizers; agents that facilitate the production of reactive oxygen species (ROS). This technique requires the uptake and retention of sonosensitizers by the cancer cells; ultrasound can then be applied to activate these sonosensitizers producing ROS and other toxic molecules.<sup>77</sup> Cavitation processes activate sonosensitizers from the ground state to the excited state. As they return to their stable ground state, energy is released that is transferred to the surrounding oxygen, producing large amounts of ROS such as oxygen ions, singlet oxygen, and peroxides. ROS are highly toxic to cells and can result in apoptosis.<sup>78</sup> Sonosensitizers have a very low risk of systemic toxicity and are considered to be safe because they only become bioactive after being exposed to ultrasound, which can be focused on the tumor without involving the surrounding tissues.<sup>79</sup>

As discussed earlier, ultrasound plays a role in enhancing cell membrane permeability (sonoporation) via microbubbles generated during the cavitation process. Sonoporation allows the transfer of molecules, including drugs and DNA, from extra- to intracellular compartments. Studies conducted both *in vitro* and *in vivo* have shown that sonoporation enhances the uptake of anticancer drugs,

e.g. bleomycin and Adriamycin.<sup>80,81</sup> Sonoporation has also been found to enhance gene uptake by cells when ultrasound (0.5-4 MHz) was applied.<sup>82</sup> As described above, ultrasound enhances the uptake of different molecules either by forming small pores in the membrane or by enhancing endocytosis.<sup>58,83</sup>

#### 4.1. Ultrasonically triggered nanoparticles for drug delivery and cancer treatment

The energy produced by ultrasound can be used as an external stimulus to trigger drug release from nanoparticles. While other external stimuli such as light penetrate poorly into the body, low-frequency ultrasound penetrates deeply into soft tissues.<sup>84</sup> The ability to focus ultrasonic waves using probes placed on the patient's skin allows the safe non-invasive deposition of significant levels of energy into specific small volumes deep inside the body while sparing

As mentioned above, inertial cavitation, high temperatures, and pressures are generated in response to the collapse of the bubbles, which in turn generate ROS.<sup>70</sup> Combining hard nanoparticles (metals and metal oxides) with ultrasound has many advantages. In addition to their possible use as drug delivery vehicles, these nanoparticles can act both as sonosensitizers (via their metal oxide surface chemistry) and as cavitation nuclei (via the reduction of the required peak negative pressures to form gas bubbles, thus increasing the number of bubbles and the cavitation rate).<sup>77</sup> Acoustic cavitation can cause structural changes in mesoporous nanoparticles by mechanically fracturing and creating fresh highly-reactive metal oxide surfaces. The ROS produced, due to the effect of both the ultrasound and the nanoparticles cause oxidative stresses that resulted in reduced cell viability due to membrane destruction, fragmentation of the DNA and damage to the mitochondrial membrane.<sup>46,88</sup>

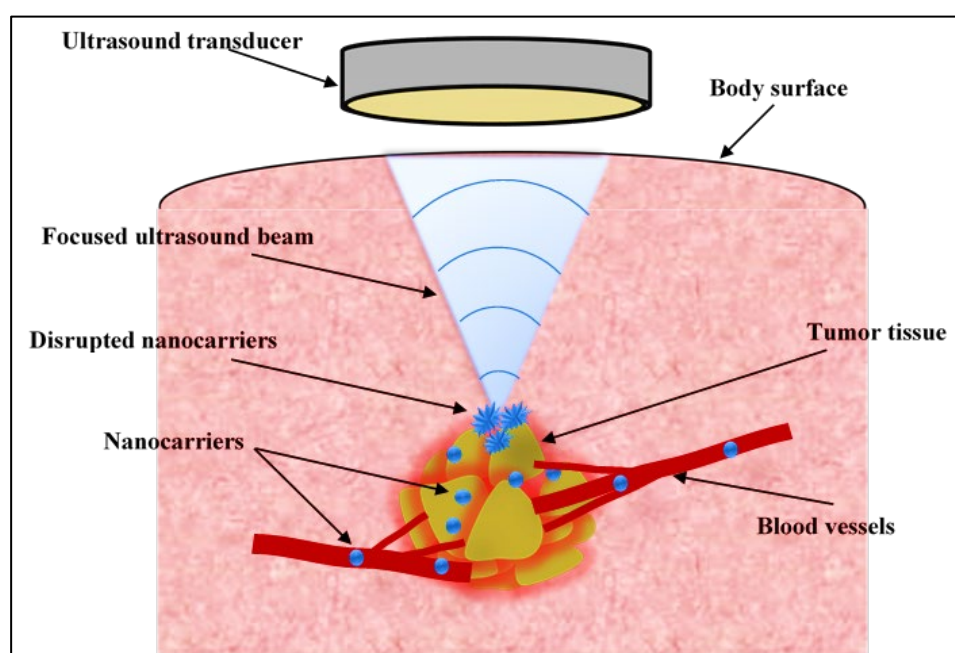


Fig. (7). Ultrasound-triggered drug release from targeted nanoparticles. The controlled ultrasound beam is focused on the tumor tissue, nanocarriers passing through the high intensity focused beam are disrupted or activated.

the surrounding healthy tissues.<sup>23</sup> The effective focus of the ultrasound can target volumes as small as a few cubic millimeters.<sup>85</sup> As shown in Figure 7, nanocarriers located in the focal zone can be triggered by the ultrasound to release their payload, while nanocarriers positioned outside this zone will not be triggered.<sup>86</sup> Ultrasonically triggered drug release from nanocarriers can occur as a result of the thermal effect of the ultrasound and/or the mechanical effect through cavitation or radiation forces. Subjecting sonosensitive nanocarriers to these physical forces induces structural destabilization and subsequent drug release. In addition, these forces induce a transient increase in blood vessel permeability, thus enhancing extravasation of particles or drugs into tumor interstitial spaces, increasing the eventual cellular uptake of the drug.<sup>32,87</sup>

##### 4.1.1. Mesoporous Silica Nanoparticles (MSNs) triggered with US

Mesoporous silica nanoparticles (MSNs) are porous silica nanoparticles with pore diameters ranging from 2 nm to 50 nm. In addition to their potential as cavitation nuclei and sonosensitizers (see above), these MSNs have been extensively investigated for their promise in drug delivery and biomedical applications.<sup>89</sup> MSNs are also biocompatible and biodegradable.<sup>90,91</sup> They have large surface areas due to their high pore volumes, which confers high loading efficiency of drugs. Horcajada et al.<sup>92</sup> reported that the rate of delivery of ibuprofen, encapsulated inside MCM 41 type mesoporous materials, decreased in response to a decrease in pore diameters from 3.6 nm to 2.5 nm. Drug solubility and interactions with pore walls determine the loading and release efficiency of the MSNs.<sup>93</sup> The pore walls can be functionalized with various chemical groups that

control both the loading and the release of the drugs by controlling the time and duration of pore opening or closure. This limits the possibility of premature drug release in the bloodstream, but allows the release of the cargo once the MSNs reach the desired site.<sup>93</sup>

Ultrasound has been used by Paris et al.<sup>94</sup> to trigger doxorubicin (DOX) release from MSNs. In their study, MSNs were grafted with temperature-sensitive copolymers (MEO<sub>2</sub>MA and THPMA) able to open the pores (the polymer having a coil-like form during drug loading), and then close the pores (polymer having a collapsed form during blood circulation). The energy of the ultrasound waves cleaves the hydrophobic tetrahydropyranil moieties changing the polymer's conformation to coil-like, which then allows drug release. A more recent study by the same group<sup>95</sup> investigated ultrasound-mediated drug release from MSNs grafted with a polyethylene glycol (PEG) shell. When high-frequency ultrasound is applied, the hydrophilic PEG shell detaches from MSNs encapsulating the drug topotecan, and the positive charge of the exposed surface led to their internalization into the human osteosarcoma cells, releasing the drug inside these cells. Li et al.<sup>96</sup> synthesized MSNs coated with the polymer sodium alginate (SA), and carboxyl-calcium (COO<sup>-</sup>-Ca<sup>2+</sup>) was used to crosslink the SA on the outer layer (SA-CaCl<sub>2</sub>), blocking the pores and preventing the release of the encapsulated drug. Upon sonication using both low-frequency (20 kHz) and high-frequency (1.1 MHz) ultrasound, the coordination bonds were destroyed and the drug was released from the MSNs. The group concluded that cavitation was the mechanism behind the disruption of these coordination bonds, and hence the subsequent drug release.

Another group<sup>97</sup> has synthesized multifunctional targeted MSNs capped with  $\beta$ -cyclodextrin ( $\beta$ -CD) and functionalized them with folic acid (FA- $\beta$ -CD) as a targeting moiety to increase uptake by cancer cells. These MSNs were loaded with the chemotherapy drug paclitaxel (PTX). To enhance their sonosensitivity, gas bubbles were stored in a hydrophobic internal channel. While these nanoparticles had slow drug release in the bloodstream, triggering with low-intensity ultrasound (0.4 to 1 W/cm<sup>2</sup>, 1 MHz) significantly enhanced drug release both *in vitro* and *in vivo*. When activated using ultrasound, MSNs act as cavitation nuclei or sonosensitizers, as explained above. The roughness of their surfaces leads to the presence of residual gas bubbles within the pores. In addition, the dissolution of the silicon nanoparticles forms hydrogen bubbles.<sup>98</sup> The synergistic cytotoxic effect of low-intensity ultrasound and MSNs has resulted in the destruction of cancer cells *in vitro*.<sup>99,100</sup>

#### 4.1.2. Super magnetic iron oxide nanoparticles triggered with US

Superparamagnetic iron oxide nanoparticles (SPIONs) are composed of magnetite iron oxide (Fe<sub>3</sub>O<sub>4</sub>) or its oxidized form maghemite ( $\gamma$ -Fe<sub>2</sub>O<sub>3</sub>), with diameters ranging between 1 and 100 nm. SPIONs consist of iron oxide cores and, can, therefore, be targeted to a specific location via externally applied magnets. A magnet is placed externally over the targeted area producing a strong magnetic field that attracts the SPIONs to the desired location. SPIONs are promising nanocarriers capable of delivering drugs to the body because they are biodegradable and simple to synthesize.<sup>101</sup>

Different types of functional groups, including carboxyl groups and carbodiimides, can be grafted on the SPION surface. Chemotherapeutic drugs can then be conjugated to these functional groups. However, because drugs are only loaded on their surface, SPIONs have been found to release their drug load soon after injection into the bloodstream (burst effect). The anti-neoplastic agents then fail to reach their therapeutic levels at the desired site. To reduce their premature drug release, biocompatible polymers are usually used to coat the metal cores. Various polymers, including PEG, polylactic-co-glycolic acid (PLGA), polyethylene-co-vinylacetate, and polyvinylpyrrolidone (PVP), have been used as coating materials in aqueous solutions.<sup>102</sup> These coatings protect the magnetic core and allow drug binding by forming covalent bonds, adsorption or entrapment on the particles.<sup>103</sup> For example, coating the iron oxide core with the cross-linked polymer, poly (ethylene glycol)-co-fumarate (PEGF), caused a significant reduction in premature release (21 %) compared to the non-coated SPIONs.<sup>104</sup> To increase their targeting abilities, the surfaces of the SPIONs can be crafted with targeting molecules such as folic acid, RGD, proteins, transferrin, and hyaluronic acid.<sup>104</sup> Several *In vitro* studies have shown no, or low, cytotoxic effects of SPIONs on cell cultures.<sup>105–107</sup> However, other *In vivo* studies showed controversial toxicity patterns of SPIONs; from negative<sup>108,109</sup> to positive toxicity<sup>110,111</sup> in several pre-clinical animal models. Generally, the toxicity of SPIONs depends on their size, dose, surface coating, and species.<sup>112</sup>

Fard et al.<sup>113</sup> investigated the effect of exposing Fe<sub>3</sub>O<sub>4</sub> nanoparticles to ultrasound (1 MHz and intensity of 2 W/cm<sup>2</sup>) on the viability of cancer cells. The study showed that the level of reactive oxygen species (ROS) in the cells was enhanced following sonication, resulting in cell destruction. Furthermore, the study also reported that high concentrations of Fe<sub>3</sub>O<sub>4</sub> nanoparticles (above 100 mg/ml) behave as sonosensitizers generating ROS (synergic effect). Coating Fe<sub>3</sub>O<sub>4</sub> nanoparticles with sonosensitizers, e.g., titanium dioxide (TiO<sub>2</sub>), is a promising technique for enhancing ultrasound-assisted stimulation by inducing the formation of ROS, including hydrogen peroxide, hydroxyl radicals, and superoxides.<sup>114</sup> A study by Shen et al.<sup>115</sup> investigated the cytotoxicity of DOX-loaded titanium dioxide-encapsulated Fe<sub>3</sub>O<sub>4</sub> nanoparticles (Fe<sub>3</sub>O<sub>4</sub>-TiO<sub>2</sub> NPs) coupled with ultrasound (1 MHz, 1 W/cm<sup>2</sup>). This study reported that these nanoparticles produced ROS following the exposure to ultrasound. Incubation of cancer cells with Fe<sub>3</sub>O<sub>4</sub>-TiO<sub>2</sub>-DOX followed by sonication showed higher toxicities compared to the treatment with free DOX or Fe<sub>3</sub>O<sub>4</sub>-TiO<sub>2</sub>-DOX alone.

#### 4.1.3. Gold nanoparticles triggered with US

Gold nanoparticles (GNPs) have intriguing potential as cancer drug nanocarriers. GNPs possess unique optical (energy absorption), physical (size and stability), and chemical (reactive with thiols) characteristics, which give them a highly multifunctional platform for imaging, guiding surgical procedures, and drug delivery.<sup>75,116–118</sup> A study by Chithrani and Chan<sup>119</sup> reported that cellular uptake of the GNPs is mainly through the receptor-mediated clathrin-dependent endocytosis pathway. The study also reported that the small diameter of the nanocarriers ( $\leq 50$ -nm) leads to faster uptake and higher concentrations of the GNPs inside the cells, relative to larger

carriers. GNPs were found to interact with heparin-binding glycoproteins, including vascular permeability factors and basic fibroblast growth factors that mediate angiogenesis. Inhibition of angiogenesis reduces tumor growth. Although GNPs themselves could be used as therapeutic agents to destroy tumor cells, they have also been used in the field of drug delivery. GNPs, with diameters of 10 to 100 nm, can be conjugated to chemotherapeutic drugs, making them potential drug delivery carriers.<sup>118</sup> The conjugation is achieved by simple physical adsorption and by using alkanethiol linkers.<sup>120</sup> To enhance their solubility and stability, GNPs can be decorated with PEG thiols (pegylation) to reduce their uptake by the reticuloendothelial system (RES). In addition, GNPs can be designed to target tumors by conjugation with various ligands such as transferrin (TF) and folic acid.<sup>121,122</sup> Once at the desired location, drug release from the GNPs can be stimulated using external (light, ultrasound, laser) or internal triggers (pH, redox condition, matrix metalloproteinase, heat).<sup>18</sup>

When ultrasound is applied, gold particles in the liquid medium act as nucleation agents, which enhances the cavitation processes by reducing the latter's threshold. When added to the culture media, GNPs were found to enhance the inertial cavitation of ultrasound.<sup>123</sup> Brazzale et al.<sup>124</sup> synthesized gold nanoparticles containing PEG as a polymer coating and folic acid as a targeting moiety (FA-PEG-GNP). Incubation of these nanoparticles with two cancer cell lines (KB and HCT-116), followed by exposure to ultrasound ( $8 \times 10^{-6}$  J cm<sup>-2</sup> and  $8 \times 10^{-5}$  J cm<sup>-2</sup>, for 5 min at 1.866 MHz) significantly reduced cell growth and proliferation together with the significant generation of ROS species. Another study by Kosheleva et al.<sup>125</sup> reported that lung cancer cells (A549) showed higher sensitivity to the treatment with GNPs combined with 4 MHz HIFU, than to the treatment with the GNPs only.

Furthermore, combining GNPs with ultrasound (1 and 3 MHz, 2 W/cm<sup>2</sup>) and an intense pulse of light was found to significantly improve the therapeutic effect in colon tumors in mice.<sup>126</sup> A study that was conducted *in vivo* by Shanei et al.<sup>127</sup> found that ultrasound (1.1 MHz, 2 W/cm<sup>2</sup>) applied to GNPs conjugated to the sonosensitizer PpIX (Au-PpIX), resulted in greater inhibition of the colon cancer (CT26) than when using PpIX alone. This was attributed to GNPs acting as nucleation agents, leading to more collapsing cavities in addition to improving uptake of the Au-PpIX by the tumor cells.

#### 4.1.4. Carbon nanotubes (CNTs) triggered with US

Over the past 20 years, many studies have shown the potential of employing carbon nanotubes (CNTs) as drug and gene delivery systems that benefit from their unique physical properties including their low mass density, large surface area, wide range of diameters (from a few to hundreds of nanometers), in addition to their non-immunogenicity, biocompatibility, and high drug cargo-carrying ability.<sup>128</sup> A CNT is a carbon allotrope consisting of a single graphene sheet rolled up to form a single-walled carbon nanotube (SWCNT).<sup>129</sup> Multi-walled CNTs carbon nanotubes (MWCNTs) contain more than one rolled sheet arranged in a concentric form.<sup>128</sup> CNTs dissolve poorly in aqueous media and tend to form aggregates. To overcome these issues, CNTs surfaces can be modified using physical or

chemical methods, including electrostatic, hydrophobic, or covalent and non-covalent bonding.<sup>129</sup> Considerable research has been conducted on their purification, carboxylation, acylation, amidation, esterification, PEGylation, and surface modification with polymers. In addition, their surfaces can be conjugated to targeting molecules including carbohydrates, proteins, antibodies and folic acid, making them suitable for targeted drug delivery.<sup>128,130,131</sup> The potential of CNTs in cancer treatment through both photothermal therapy and photodynamic therapy have been investigated. CNTs have been found to be capable of transforming near-infrared light into heat which established their role in photothermal therapy through promoting hyperthermia (thermal ablation) leading to enhanced tumor suppression.<sup>132</sup> Combining CNTs with photosensitizers (PS) that generate ROS upon illumination resulted in a noticeable tumor reduction in mice.<sup>133</sup>

In addition to their drug loading capabilities, CNTs can be engineered to act as excellent adjuvant contrast agents for use in imaging.<sup>129</sup> For example, the hyperechogenicity of the MWCNTs promoted their use as ultrasound contrast agents.<sup>134,135</sup> A study by Delogu et al.<sup>136</sup> reported that functionalized MWCNTs have long-lasting ultrasound contrast properties. Pagani et al.<sup>137</sup> reported that the cavitation formed during sonication results in the dispersion of CNTs in liquids by exfoliating CNTs bundles into individual units, in addition to the breaking and shortening of the individual CNTs. Spectroscopic and morphological analysis of CNTs subjected to sonication using an ultrasonic bath (water volume 2.5 L, power 260 W) revealed that as sonication time increased, the length of CNTs' decreased dramatically.<sup>138</sup> In addition, as the length of CNTs decreased due to the increase in sonication time, the structures of CNTs also changed from solid-like to liquid-like structures.<sup>139</sup> An earlier study by Ruan and Jacobi<sup>140</sup> reported that the ability of MWCNTs to conduct heat increased nonlinearly with an increase in sonication specific energy input.

The ability of ultrasound to successfully disperse CNTs, releasing their load in a controlled manner, makes ultrasound-assisted CNT drug delivery a promising technique in cancer treatment. In addition, the increased thermal conductivity of MWCNTs following sonication shows the potential of combining MWCNTs with HIFU ablation. More research is certainly needed to develop the role of ultrasound-assisted CNTs in drug delivery and to optimize suitable sonication parameters to ensure the successful outcome pertaining to the desired ultrasound-mediated effect. However, there is considerable concern about the biocompatibility and toxicity of MWCNTs and they have recently been added to the SIN List as a nanomaterial of very high concern.<sup>141</sup>

#### 4.1.5. Polymeric micelles triggered with ultrasound

Polymeric micelles are nanocarriers synthesized from amphiphilic copolymers forming a hydrophobic core and a hydrophilic shell. Polyethylene glycol (PEG) is widely used to form the hydrophilic outer shell while polyesters, polyethers, or polyamino acids are used as the blocks forming the hydrophobic core.<sup>142</sup> Polymeric micelles spontaneously self-assemble when in aqueous solutions to form a stable and unique nanoscale structure with many physicochemical and biological advantages, making them efficient drug delivery

vehicles.<sup>143</sup> The hydrophilic shell increases the circulation time in the blood while evading the uptake of the polymeric micelles by the immune cells, thus reducing their clearance from the blood. The hydrophobic core ensures that drugs insoluble in aqueous solutions can easily be encapsulated and delivered to the cancer site.<sup>143</sup> In addition to the physical entrapment of the drugs inside their cores, drugs can be loaded into polymeric micelles through chemical conjugation and ionic bonding. Micelles can also be crafted with a number of targeting moieties, including antibodies, folic acid, growth factors, and transferrin.<sup>144</sup> Upon reaching the desired site, intrinsic or extrinsic stimuli can be used to trigger drug release from micelles with temporal and spatial control.

Different studies have explored ultrasound to trigger the controlled release of active agents from polymeric micelles, mainly Pluronic micelles.<sup>145–147</sup> Ultrasound can trigger irreversible drug release from polymeric micelles through ester hydrolysis which is usually associated with HIFU (1.1 MHz); low-frequency ultrasound (20–90 kHz), on the other hand, triggers reversible drug release through inertial cavitation.<sup>148</sup> Xuan et al.<sup>149</sup> showed that the effect of HIFU could be boosted through the incorporation of a small amount of HIFU-labile 2-tetrahydropyranyl methacrylate (THPMA) comonomer units into the core of the micelles to enhance their thermosensitivity, thus releasing more encapsulated drugs with HIFU irradiation. Cavitation triggers the release of the drugs from the core of polymeric micelles by disrupting the assembled polymeric micelles,

releasing their payload. When ultrasound is paused, polymeric micelles have the ability to reassemble and successfully re-encapsulate the drugs inside their cores. Therefore, the reversible disordering of the micelles can produce reversible drug release.<sup>146,147</sup> Wu et al.<sup>150</sup> recently reported that P123/F127 mixed micelles, loaded with curcumin, circulated in the blood for longer periods, showing higher uptake by cancer cells compared to free curcumin. The study reported the cleavage of the Cu(II)–terpyridine dynamic bond in the copolymer chain when exposed to HIFU (3 W, 1.90 MHz) for 3 min, resulting in the disruption of the micellar structure and subsequent drug release. Salgarella et al.<sup>148</sup> investigated micelles prepared using five different types of poly(2-oxazoline) block copolymers and found that sonication (40 kHz, 20 W, 10 min) enhanced the release of the encapsulated dexamethasone from 6 % to 105 %. The study found that the type of copolymer used had an effect on the amount of drug released. Table 1 below shows a summary of some studies investigating the ultrasound-mediated drug release from polymeric micelles.

Table 1. Studies investigating the acoustically triggered drug release from polymeric micelles.

Reference	Study type	US parameters	Encapsulated substance	Effect
Liang et al. <sup>151</sup>	<i>in vitro</i> study	1.1 MHz. (0–150 W)	Pyrene/Nile red	The encapsulated agents are quickly released from the (PPG-[Cu]-PEG) micelles following sonication using HIFU.
Staples et al. <sup>152</sup>	<i>in vivo</i> study using DHD/K12/TRb colorectal epithelial cancer	20 kHz (1.0 W/cm <sup>2</sup> ) or 476 kHz (23.61 W/cm <sup>2</sup> )	DOX	US increased DOX concentration by about 50% in the tumor. Varying the frequency had no statistical difference on the treatment.
Hasanzadeh et al. <sup>153</sup>	<i>in vivo</i> using murine spontaneous breast adenocarcinoma	3 MHz (2 W/cm <sup>2</sup> ) and 28 kHz (0.04 W/cm <sup>2</sup> )	DOX	Both frequencies used triggered drug release in addition to enhancing the uptake of the drug by the cancer cells
Rapoport. <sup>154</sup>	<i>in vitro</i> study using Ovarian carcinoma A2780 and MDR cells	(1, 3 MHz) and (20 kHz–3 MHz) power densities (0.058, 6 and 0–0.2 W/cm <sup>2</sup> )	DOX	Sonication enhanced drug release from micelles, as well as enhancing the intracellular uptake of the drug.
Nelson et al. <sup>155</sup>	<i>in vivo</i> study using Colon tumor (DHD/K12/TRb)	20 and 70 kHz (0.048, 1 and 2 W/cm <sup>2</sup> )	DOX	US enhances DOX release from micelles. US may assist drugs/micelles uptake by the cancer cells.
Husseini et al. <sup>156</sup>	<i>in vitro</i> study	20 to 90 kHz (0 to 3 W/cm <sup>2</sup> )	DOX and Ruboxyl	Cavitation disrupted the micelles releasing their encapsulated drugs. DOX release was higher than that of Ruboxyl.

Munshi et al. <sup>157</sup>	<i>in vitro</i> study using HL-60 human leukemia cells	80 KHz (3.6 W/cm <sup>2</sup> )	DOX	Sonication resulted in lowering DOX IC <sub>50</sub> from 2.35 µg/ml to 0.19 µg/ml.
Zeng and Pitt <sup>158</sup>	<i>in vitro</i> study	Low-frequency US (70 kHz)	DPH/ DOX	DOX release increased as the temperature increased from 25 °C (2 %) to 37 °C (4 %). Dox re-encapsulation occurred when sonication was paused.
Marin et al. <sup>159</sup>	<i>In vitro</i> study using HL-60 Human Leukemia, breast cancer (MCF-7) and MDR cells	20-kHz (0.058 W/cm <sup>2</sup> ), 67-kHz (2.8 W/cm <sup>2</sup> ) and 1.0-MHz (7.2 W/cm <sup>2</sup> )	DOX	DOX release was increased at higher power densities.
Marin et al. <sup>160</sup>	<i>In vitro</i> study using HL-60 Human Leukemia cells	20 kHz (1.4, 14 and 33 mW/cm <sup>2</sup> )	DOX	Sonication resulted in enhancing DOX uptake by the cancer cells.
Gao et al. <sup>161</sup>	<i>in vivo</i> study using Ovarian carcinoma A2780 cells	1 MHz or 3 MHz (3.4 W/cm <sup>2</sup> )	DOX	Sonication of the drug-loaded micelles inhibited tumor growth.
Husseini et al. <sup>162</sup>	<i>in vitro</i> study	70 kHz (0.28 W/cm <sup>2</sup> )	DOX	Transient cavitation disrupted and disassembled the micelles, thus releasing the encapsulated drug.
Husseini et al. <sup>163</sup>	<i>in vitro</i> study using HL-60 human leukemia cells	70 kHz, (1.3, 2.3 W/cm <sup>2</sup> )	DOX	US-mediated drug release from micelles resulted in cell death through apoptosis.
Zhang et al. <sup>164</sup>	<i>in vitro</i> study	High-intensity US	Nile red	Collapsed cavitation occurring at the focal point of HIFU resulted in the irreversible release of Nile Red from micelles.
Husseini et al. <sup>165</sup>	<i>in vitro</i> study using HL-60 human leukemia cells	70 kHz, (1.3 W/cm <sup>2</sup> )	DOX	US triggered DOX released from Pluronic P105 micelles damaging the DNA of HL-60 cells in the process.
Pruitt and Pitt <sup>166</sup>	<i>in vitro</i> study using HL-60 Human leukemia cells	70 kHz (1.5 W/cm <sup>2</sup> )	DOX	US enhanced DOX toxicity by extravasation, perturbation of the cell membrane, and permeabilization of micellar membranes.
Husseini et al. <sup>167</sup>	<i>in vitro</i> study using HL-60 cells/HeLa cells	70 kHz, (1.2 W/cm <sup>2</sup> )	DOX	The application of US enhances drug uptake through the cell membrane, not through the acidic vesicles.
Husseini et al. <sup>146</sup> ; Husseini et al. <sup>168</sup>	<i>in vitro</i> study	70 kHz (0.53 W/cm <sup>2</sup> -6 W/cm <sup>2</sup> )	DOX	Maximum DOX release (14%) was measured at 5.4 W/cm <sup>2</sup> following a zero-order model
Tong et al. <sup>169</sup>	<i>in vitro</i> study	1.1 MHz (0-150 W)	Pyrene/DTT	Combining the effect of HIFU and redox enhanced drug release from copolymer micelles.
Husseini et al. <sup>170</sup>	<i>in vitro</i> study	70 kHz (0.27 W/cm <sup>2</sup> )	DOX	Micelles are triggered to release their load as a result of the shearing events produced by cavitation.

#### 4.1.6. Liposomes triggered with ultrasound

Liposomes are nano-sized carriers that contain central aqueous compartments surrounded by a lipid bilayer shell. Liposomes are able to efficiently entrap hydrophobic drugs within the lipid bilayer and encapsulate hydrophilic drugs in their cores.<sup>171</sup> Monodisperse liposomes with an optimized diameter (less than 200 nm) can be manufactured, which allows them to extravasate through the leaky vasculature of solid tumors. Surface modification of the liposomes with polymers such as polyethylene glycol (PEG), known as Stealth<sup>®</sup> liposomes, have reduced uptake into the cells of the RES, and longer circulation times than liposome lacking this modification.<sup>150,172</sup> Drug encapsulation inside the liposomes can significantly increase the accumulation of the loaded drugs at the sites of solid tumors showing a 50- to 100-fold increase compared to the free drug.<sup>173,174</sup> However, this does not mean an equally significant increase in therapeutic effects, as the drugs have to be released from the carriers before they can act on the surrounding cells.

Drug delivery of anthracycline-containing liposomes have been studied widely in the literature since several of these are already approved by the FDA including liposomal doxorubicin (Myocet<sup>™</sup>), pegylated liposomal doxorubicin (Doxil<sup>®</sup> also known as Caelyx<sup>™</sup>), liposomal daunorubicin (DaunoXome<sup>®</sup>)<sup>175</sup> and one generic liposomal doxorubicin Lipodox<sup>®</sup>. For tumors with highly permeable vasculature, e.g., Kaposi's sarcoma, these anthracycline-liposomes are capable of selectively delivering high dosages of anthracyclines to tumor tissues without harming healthy, drug-sensitive tissues such as heart tissue. This is due to their high encapsulation and retention efficacy, as well as their prolonged circulation time in the bloodstream.<sup>176,177</sup> In addition, the small size of the liposomes allows them to escape through the defective vasculature surrounding the tumor (EPR effect) and accumulate in large numbers at the diseased location.<sup>178</sup> However, as long as DOX is encapsulated inside the liposomes, it remains in a crystalline form and is not bioavailable, so the concentrations of free (bioavailable) drugs at the tumor site will be sub-optimal.<sup>179</sup>

Ultrasound has been combined with liposomes in several studies. Low-frequency ultrasound (LFUS) enhances the permeability of cell membranes, thus enhancing drug and gene uptake.<sup>180</sup> As the phospholipid bilayer structure surrounding the liposomes is similar to that of the cells, LFUS application also enhances the permeability of liposomes, thus increasing the rate of content release.<sup>144</sup> Several studies, conducted *in vitro*, have reported that LFUS (20 kHz) enhanced drug release from liposomes.<sup>181,182</sup> *In vivo* studies have reported enhanced therapeutic benefits of combining US and liposomal cytostatic drugs in tumor treatment.<sup>183,184</sup> Liposome sensitivity to the acoustic waves is affected by their lipid composition. For example, the sonosensitivity of HSPC-based (solid) liposomes is lower than that of DOPE-based (fluid) liposomes, the latter being highly sonosensitive, releasing their payload efficiently due to the irreversible disruption of the membrane during sonication.<sup>183</sup> Furthermore, DSPE-based liposomes released more DOX compared to DSPC-based liposomes (69% and 9% respectively) following 6 min of insonation.<sup>182</sup> Liposomes prepared from DOPE/DSPC/DSPE-PEG2000/cholesterol (25:27:8:40 mol%) have

extended circulation times and released 70% of their contents following 6 min of sonication.<sup>185</sup>

The sonosensitivity of liposomes can be further enhanced by the internal incorporation of a gas. Emulsion liposomes (eLiposomes) can encapsulate perfluorocarbon nanodroplets.<sup>186</sup> The energy of the US wave causes the evaporation and expansion of the gas, thus rupturing the liposomes (drug release) and promoting sonoporation (drug uptake). Emulsion liposomes are stable at physiological temperatures.<sup>187</sup> Sonication for 15 min (1 W/cm<sup>2</sup>) has resulted in the total destruction of eLiposomes.<sup>188</sup>

Following sonication, free DOX injected together with eLiposomes significantly inhibited the growth of osteosarcoma cells achieving similar therapeutic effects to that of free DOX but at a much lower dose (1/5 the dose of free DOX).<sup>189</sup>

Thermo-responsive liposomes are sensitive to increases in temperature and can be triggered to release their load when exposed to mild hyperthermia. Thermodox<sup>®</sup>, temperature-sensitive liposomes (TSLs) encapsulating DOX, reached Phase III clinical trials but failed to meet the primary endpoint of a 33% improvement in progression-free survival.<sup>190</sup> TSLs release their payload when the local temperature reaches their membrane solid to fluid transition temperature ( $T_m$ ), at which point their fluidity changes from a solid-like phase/structure to a liquid-crystalline phase/structure.<sup>191</sup> As tumors are often warmer than healthy tissue, this is a form of triggered release.

There is interest in applying US with TSLs that have a  $T_m$  slightly higher than physiological temperatures for controlled drug release. Usually, a mild rise in local heat (mild hyperthermia) is achieved using medium frequency ultrasound; overheating can be avoided by controlling the duty cycle.<sup>192</sup> Farr et al.<sup>193</sup> reported that temperature-sensitive liposomes encapsulating DOX (TSL-DOX), triggered by the mild hyperthermia, produced by HIFU, increased DOX uptake by mouse pancreatic tumor tissue by 23-fold compared to TSL-DOX alone. Temperature-sensitive liposomes encapsulating DOX combined with US and microwave triggering were used to treat breast cancer patients, showing significant improvement (48 %) in local response.<sup>194</sup> A recent clinical trial<sup>195</sup> used thermosensitive liposomes combined with focused ultrasound to deliver DOX to patients with liver tumors. The trial concluded that while HIFU-triggered TSL-DOX enhanced drug delivery to the tumor, no adverse effects were observed as a result of the thermal ablation produced by HIFU. Table 2 below shows a summary of studies investigating the acoustically triggered drug release from liposomes.

Table 2. Studies investigating the acoustically triggered drug release from liposomes.

Reference	Study type	US parameters	Encapsulated substance	Effect
Rizzitelli et al. <sup>196</sup>	<i>In vitro/in vivo</i> study using TS/A (mammary) cells	3 MHz (3.3 W/cm <sup>2</sup> )	DOX	Enhanced therapeutic outcome due to the improved drug diffusion in the tumor following sonication.
Dromi et al. <sup>197</sup>	<i>In vitro/in vivo</i> study using murine adenocarcinoma tumors	1.189 MHz (4 W/cm <sup>2</sup> )	DOX	Combining HIFU with TSLs enhanced DOX delivery.
Kheirilomoom et al. <sup>198</sup>	<i>In vivo</i> study using Murine breast cancer	1.54 MHz	DOX	Tumor elimination following the treatment with ultrasound triggered liposomal copper-DOX, CuDOX-LTSLs.
Lattin et al. <sup>199</sup>	<i>In vitro</i> study	20 kHz (5 W/cm <sup>2</sup> )	Calcein	Following sonication, calcein release was significantly higher from e-Liposomes compared to conventional liposomes.
Gray et al. <sup>195</sup>	Phase I Trial	0.96 MHz	DOX	TSL combined with focused ultrasound hyperthermia is feasible and safe.
Um et al. <sup>200</sup>	<i>In vitro</i> study using EMT6 mouse mammary tumor cells	15 kHz (20 W/cm <sup>2</sup> , 10 W/cm <sup>2</sup> and 10 $\mu$ W/cm <sup>2</sup> )	DOX	Similar enhancement of DOX release from thermosensitive liposomes triggered with both thermal and non-thermal acoustic treatment.
Santos et al. <sup>201</sup>	<i>In vivo</i> study using Human FaDu squamous cell	1.2 MHz	DOX	Combining TSL and Focused US improved drug delivery.
Awad et al. <sup>202</sup>	<i>In vitro</i> study using breast cancer cell lines (MDA-MB-231 and MCF-7)	20 kHz (6,7 and 12 W/cm <sup>2</sup> ) and 40 kHz (1 W/cm <sup>2</sup> )	Calcein	Calcein uptake by cancer cells was enhanced following sonication.
Lentacker et al. <sup>203</sup>	<i>In vitro</i> study using Melanoma cells	1 MHz (2 W/cm <sup>2</sup> )	DOX	Following the exposure to US, DOX-liposomes containing microbubbles were more effective in tumor elimination.
Yang et al. <sup>204</sup>	<i>In vivo</i> study using (GBM) 8401 glioma cells	1 MHz (2.9 W/cm <sup>2</sup> )	DOX	Sonication enhanced targeted drug delivery of AP-1 Lipo-DOX, resulting in the inhibiting the brain tumor growth.
Novell et al. <sup>205</sup>	<i>In vitro</i> study	1 MHz	Calcein	The mechanical stresses generated by the focus US enhanced drug release from TSLs.
Treat et al. <sup>206</sup>	<i>In vivo</i> study using 9L gliosarcoma cells	1.7 MHz	DOX	Combining the US-mediated BBB disruption increased the therapeutic effect of liposomal DOX in the brain.
Park et al. <sup>207</sup>	<i>In vivo</i> study using HeLa cells	1 MHz	DOX	HIFU combined with the TSL liposomes significantly inhibited tumor regression.
Pitt et al. <sup>208</sup>	<i>In vivo</i> study using Colorectal cancer cells (DHD/K12/TRb)	20 kHz (1 W/cm <sup>2</sup> )	DOX	US combined with DOX-liposomes showed a higher reduction of tumor growth compared to DOX delivered from micelles.

Ahmed et al. <sup>29</sup>	<i>In vitro</i> study	20 kHz 1, and 3 MHz with different power densities	Calcein	Calcein release was higher at the low frequency (20 kHz) investigated.
Eggen et al. <sup>209</sup>	<i>In vivo</i> study using Prostate cancer cells	1 MHz and 300 kHz	DOX	Both frequencies used led to an increase in tumor uptake of DOX from sonosensitive liposomes.
Ranjan et al. <sup>210</sup>	<i>In vivo</i> study using Vx2 tumor cell	MR-HIFU	DOX	Following sonication, DOX delivery from LTSL to Vx2 tumors in rabbits was 3.4-fold higher than that of LTSL alone.
Salkho et al. <sup>211</sup>	<i>In vitro</i> study using breast cancer cell lines MDA-MB-231 and MCF-7	20 kHz, 1.07 and 3.24 MHz	Calcein	The exposure to LFUS revealed an enhanced calcein uptake by the cells.
Shen et al. <sup>115</sup>	<i>In vivo</i> study using human glioblastoma cell line U87 MG	1.1 MHz	Paclitaxel	Combining PTX-liposomes with US in the presence of microbubbles enhanced drug efficacy towards glioblastoma.
Aryal et al. <sup>212</sup>	<i>In vivo</i> study using rat gliosarcoma cells	690 kHz	DOX	US enhanced the delivery of liposomal DOX from pegylated liposomes.
Afadzi et al. <sup>53</sup>	<i>In vitro</i> study using HeLa cell line (cervical cancer)	300 kHz	DOX	Sonication of DOX liposomes and microbubbles enhanced DOX uptake by cancer cells.
Williams et al. <sup>213</sup>	<i>In vitro</i> study using KB-V1 (Dox resistant) and KB-3-1 (Dox sensitive) cell lines	20 kHz (1 W/cm <sup>2</sup> )	DOX	US released 78% of the encapsulated DOX from folate eLiposomes (feLD). US had no effect on the viability of both cell lines following the treatment with feLD.
Centelles et al. <sup>214</sup>	<i>In vitro/in vivo</i> study using IGROV-1 (ovarian cancer) cells	1.3 MHz	Topotecan	Enhanced uptake of both Topotecan and TSLs due to the focused US treatments.
Ueno et al. <sup>189</sup>	<i>In vivo</i> study using murine osteosarcoma cell line LM8	1 and 2 MHz (0.5 and 2 W/cm <sup>2</sup> )	DOX	The therapeutic effect of DOX was significantly improved following sonication in the presence of bubble liposomes.
Lin et al. <sup>215</sup>	<i>In vitro</i> study using HeLa cell line	20 kHz (1 W/cm <sup>2</sup> )	DOX	Higher DOX release from eLiposomes was observed following sonication when compared to liposomes without emulsions.
Hamano et al. <sup>216</sup>	<i>In vitro</i> study using 293T human embryonic kidney carcinoma cells	2 MHz (0.25-1 W/cm <sup>2</sup> )	DOX	The combination of DOX-liposomes with bubble liposomes showed a US-enhanced drug release.
Awad et al. <sup>217</sup>	<i>In vitro</i> study	20 kHz (6, 7 and 12 W/cm <sup>2</sup> )	Calcein	HSA-PEG and Tf-PEG liposomes were more sonosensitive compared to the control pegylated liposomes upon exposure to LFUS.

#### 4.1.7. Liposomes-microbubble conjugates triggered with US

Contrast agent microbubbles are widely used in diagnostic imaging. These consist of an outer shell prepared from a lipid monolayer or albumin surrounding a low-solubility gas, thus enhancing blood-to-tissue contrast.<sup>218</sup> Microbubbles have a therapeutic potential in the field of gene therapy and drug delivery.<sup>219,220</sup> Microbubbles are 1-2  $\mu\text{m}$  in diameter and usually contain a perfluorocarbon (PFC) or  $\text{SF}_6$  gas. The density of the encapsulated gas is very different from that of the surrounding water, which makes the lipid-shelled microbubbles more sensitive to the pressure generated by the ultrasound waves and highly echogenic, allowing the easy manipulation of the microbubbles using the acoustic radiation force.<sup>221</sup> Subjecting the microbubbles to the pressure produced by ultrasound ( $\text{MI} > 0.3\text{--}0.6$ ) will generate mechanical stresses as the microbubbles rapidly expand, contract or collapse. This oscillation or collapse creates micro-streaming or a local microjet, resulting in membrane permeability via sonoporation. This will significantly enhance drug and gene delivery to the cells.<sup>222</sup>

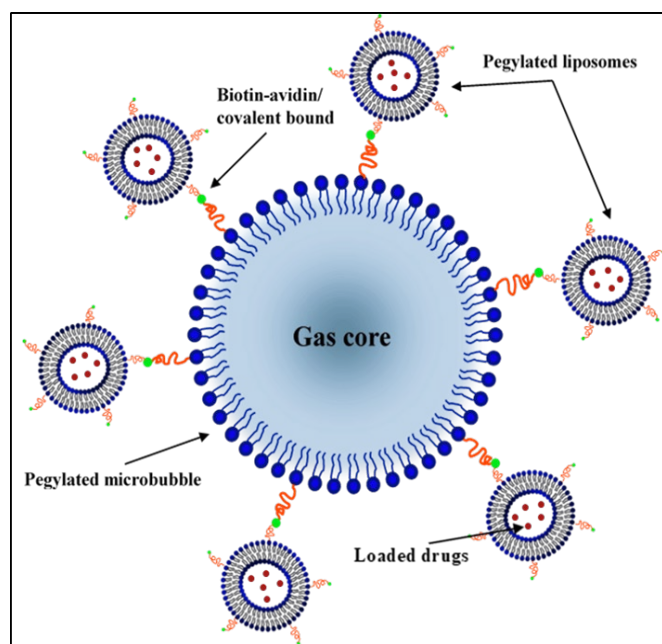


Fig. (8). Microbubble-conjugated liposomes.

Microbubbles can be used to deliver hydrophobic drugs within the protective lipid monolayer that covers them.<sup>223</sup> Generally, however, the space available for the drugs within the surrounded shell, as well as the gaseous core, is restricted which limits the efficiency of using microbubbles in drug delivery. To enhance their load capacity, microbubbles can be combined with other nanocarriers loaded with therapeutics. For example, liposomes encapsulating drugs can be conjugated to the surfaces of the microbubbles (Figure 8). These liposome-microbubble conjugates are promising drug delivery

vehicles when combined with ultrasound-triggered drug release under ultrasound imaging guidance to treat solid tumors. At low intensity, microbubbles can be positioned spatially using radiation forces.<sup>40</sup> As the intensity of the ultrasound increases, the oscillation of the microbubbles increases, leading to the total collapse and destruction of the microbubble. These physical effects increase the permeability of cancer cells and their surrounding vasculature, leading to the enhanced uptake of drugs released in the vicinity of the target cells.<sup>23</sup> Usually, the pressure produced from the collapsing microbubble disrupts the structure of the conjugated liposome located within 40  $\mu\text{m}$ .<sup>23</sup>

Drug-loaded liposomes can be conjugated to the surface of microbubbles using biotin-avidin linkers or covalent thiol-maleimide linkages.<sup>223–225</sup> Once injected into the bloodstream, microbubbles can be traced using conventional ultrasound contrast imaging modes. Following the accumulation of the liposome-microbubbles at the tumor site, high-intensity therapeutic ultrasound initiates microbubble destruction, drug release, and the sonoporation of the cells in its acoustic field.<sup>224,226</sup>

A recent *in vivo* study by Zhang et al.<sup>227</sup> reported that iRGD-targeted paclitaxel-loaded liposomes were conjugated to the surface of microbubbles using biotin-avidin linkages. The prepared iRGD-PTX liposome-microbubble complex retained ultrasound imaging capabilities and showed active ultrasound-triggered drug release. Histological examination showed elevated drug concentrations inside the cancer cells together with an increased number of apoptotic tissues in tumor xenografts leading to the inhibition of tumor growth. Another *in vivo* study by Yan et al.<sup>228</sup> reported enhanced antitumor efficacy as a result of breast tumor sonication following prior injection with paclitaxel-loaded liposomes conjugated to microbubbles, when compared to both the non-sonicated tumors and the non-conjugated liposomes. Yu et al.<sup>229</sup> reported that non-inertial ultrasound exposure released ~70% of the DOX encapsulated inside liposomes conjugated to polymer microbubbles. The study found that ultrasound exposure increased DOX uptake by the cancer cells and subsequently reduced their proliferation at 48 h.

## 5. Challenges and future perspectives of nanocarriers in cancer treatment

The development of a wide range of nanocarriers has revolutionized drug delivery in cancer treatment. Conventional chemotherapeutic drugs are faced with a number of challenges such as insolubility, short half-life, drug resistance, as well as their lack of specificity, which results in delivering toxic doses to healthy tissues. The developed nanocarriers are designed to circumvent these challenges by taking control of the drugs' circulation, distribution, and release, enhancing drug efficacy while reducing toxicity and the multidrug resistance (MDR) developed by the cancer cells. MDR is a considerable barrier in cancer treatment, and numerous studies have been dedicated to better understand MDR and develop strategies to

overcome this biological phenomenon. The proposed strategies include nanocarriers, RNA interference (RNAi) therapy, and physical approaches. The potential of nanocarriers in overcoming MDR lies in their ability to increase drug uptake and accumulation in tumor cells, suppress MDR proteins (such as the membrane bound drug transporter P-gp), and induce apoptosis.<sup>230</sup> RNAi therapy involves the use of various small interfering RNAs (siRNAs) to overcome MDR by silencing MDR genes such as P-gp/MDR1, MRP1, Bcl2, BCRP. However, the standalone therapeutic efficacy of these constructs was not satisfactory because RNAi mediators, such as siRNAs, are highly susceptible to rapid renal clearance, degradation by endogenous RNases, and recognition by innate immune receptors.<sup>231</sup> Therefore, combining nanocarriers with RNAi therapy is currently one of the most promising methods to reduce drug resistance. The success of this approach is attributed the ability of nanocarriers to prevent the rapid degradation of siRNA molecules in serum, increase target selectivity, and increase cellular uptake.<sup>230,232</sup> A few siRNA-based anticancer drugs have entered early phase clinical trials, and the majority of these studies utilized moiety-free lipid nanoparticles (LNPs) and polymeric NPs.<sup>233,234</sup> The conducted studies have shown that the developed therapeutics were relatively well tolerated, cytokine release and infusion-related side effects were manageable using supportive treatments; in addition, none of the developed systems showed any major signs of antibody-mediated rapid clearance after multiple dosing.<sup>231,233</sup> Another approach in RNAi therapy involves combining chemotherapeutics with suitable siRNAs to overcome MDR and enhance the therapeutic efficacy of chemotherapeutic agents.<sup>230,231</sup>

With respect to physical strategies, temperature and ultrasound are external stimuli that have shown great promise in enhancing the delivery of numerous nanocarriers.<sup>230</sup> Effects mediated by hyperthermia include protein denaturation, activation of apoptotic pathways, alterations in the tumor microenvironment, modifications in oxygen and nutrient distribution at the tumor site, increase in the drug uptake, and reduction in cell membrane localization of MDR proteins.<sup>230,232</sup> Ultrasound, on the other hand, can be used either to induce hyperthermia or to reverse MDR by increasing drug diffusion, increasing drug-release from nanocarriers, and increasing the cellular accumulation of therapeutic agents at the tumor site.<sup>230,235</sup> Because ultrasound has shown great promise as a triggering mechanism, a great deal of attention has been placed on the optimization of ultrasound parameters, namely frequency, intensity, and exposure duration. Some studies reported that frequencies in the order of kHz induced more release than those in the order of MHz, this was attributed to the higher attenuation of ultrasound waves experienced at higher frequencies.<sup>235</sup> Other studies have shown a linear dependence of drug release on ultrasound intensity, highlighting the importance of inertial cavitation in drug release.<sup>156,208,236</sup> With regard to duration, it has been concluded that drug release increased with increasing exposure time.<sup>235,237</sup> This was ascribed to the self-sealing properties of liposomes; as some reports suggest that lipid membranes reseal rapidly following sonoporation, but the longer the pulse duration the more time it takes for the membrane to reseal itself.<sup>238</sup> Despite the breakthroughs in research investigating ultrasound-mediated liposomal release, there is still a need for further investigations into the optimization of ultrasound

parameters in order to enable this technology to reach clinical settings.

Tumor metastasis is another major hurdle in cancer treatment. Many efforts are dedicated to developing nanocarrier-enabled tumor metastasis treatments. So far, the devised strategies can be divided into primary cancer targeting drug delivery and cancer metastasis-targeting drug delivery.<sup>239,240</sup> Primary cancer targeting drug delivery depends on preventing metastasis by inhibiting the growth of the primary tumor.<sup>240,241</sup> An emerging approach in this field targets cancer stem cells (CSCs). CSCs are a group of cells with high self-renewal abilities, which is believed to promote tumor development, recurrence and metastasis.<sup>242,243</sup> Studies have reported that reducing CSC-like properties of cancer cells or reducing the number of CSC cells can kill primary tumors and inhibit metastasis.<sup>240,242</sup> Another strategy involves targeting transcription factors (e.g. Oct-4, Nanog, KLF4, and MYC), intracellular signalling pathways (e.g. NF- $\kappa$ B, Hh, JAK-STAT, PI3K/AKT/mTOR, TGF/Smad, and PPAR), as well as extracellular factors (e.g. the vascular microenvironment, tumor associated macrophages, cancer-associated fibroblasts and mesenchymal cells, and the extracellular matrix) that regulate CSCs to inhibit tumor metastasis.<sup>239,240,242</sup> However, some issues need to be resolved before CSCs can be effectively used in cancer therapy. For instance, the characteristics of many CSCs specific to certain types of tumors are not well identified, most studies are performed in immune-deficient mice which does not mirror the biological complexity of tumors encountered when treating cancer patients. CSCs reside in niches (anatomically distinct regions within the tumor microenvironment) which are not well understood at the moment. In addition, most studies use isolated CSCs, which lack their specific niche that sustains their survival, which again does not reflect the conditions encountered when transitioning to clinical experiments.<sup>242–244</sup>

The most common approach in cancer metastasis-targeted drug delivery is the functionalization of nanocarriers with multiple targeting ligands. Another promising approach is the use of biomimetic NPs. Biomimetic NPs are a class of NPs that combine the functionality of biomaterials with the versatility of NPs to navigate complex biological systems.<sup>245</sup> NPs camouflaged in cell membranes are a novel class of biomimetic nanocarriers that can mimic some of the membrane functions of the cells from which these membranes are derived. Various cell membranes derivatives have been tested including those from red blood cells (RBCs), immune cells, macrophages, and cancer cells. Cancer cell membrane coated nanoparticles (CCMCNPs) consist of a NP core coated with a cancer cell plasma membrane. The NP core can be loaded with imaging and/or therapeutic agents, while the outer coating can carry tumor-specific receptors and antigens for cancer targeting.<sup>240,245,246</sup> CCMCNPs operate by actively reducing the ability of fibroblasts to attract cancer cells, therefore significantly reducing metastasis.<sup>245</sup> Other techniques investigated for cancer-metastasis targeted drug delivery involve targeting pre-metastasis niches.<sup>240</sup> Tumors can alter microenvironments in distant organs before their arrival at these sites, creating environments favorable for their survival and outgrowth. Pre-metastasis niche formation includes the induction of vascular leakiness, remodelling of the cell stroma and extracellular

matrix, as well as systemic effects on the immune system. The use of nanocarriers to identify such pre-metastasis niches could revolutionize cancer treatment and lead to the development of treatments that can pre-empt metastasis.<sup>240,247</sup>

Tumors vary in their biology and physiology from one patient to another, thus adding to the complexity of their treatment.<sup>248</sup> Precision and personalized medicine (PPM) is a novel approach in which treatments are tailored specifically for each individual.<sup>249</sup> In cancer therapy, PPM can be used to create individualized treatments based on the patient's tumor molecular profile.<sup>250,251</sup> Another aspect of PPM that may lead to improved disease outcomes is the use of multifunctional nanocarriers. These nanocarriers can be employed in the early detection of cancer by acting as imaging agents while delivering the drugs at the same time. The use of nanocarriers will provide the imaging of deep tissues allowing the early detection of small-sized tumors; as well as an assessment of the tumor microenvironment (namely vasculature and hypoxia) which provides information that may help predict drug behavior and allow better drug selection.<sup>252,253</sup>

Despite the promising opportunities presented by nanocarriers and their fast progress in the field of drug delivery, their clinical approval is comparatively slow, and only a few nanocarriers are commercially available such as liposomes and micelles. The future of nanocarriers depends on addressing some challenges which the technology is still facing. The efficient characterization of the different types of nanocarriers, as well as their successful reproducibility, large scale production and addressing their safety concerns are essential for their clinical development.<sup>254</sup>

The use of nanocarriers for drug delivery is relatively new compared to conventional chemotherapy. Therefore, the long term side effects/toxicities are still unknown. *In vitro* studies are essential in establishing proofs-of-concept but are not able to mimic the conditions inside the body. *In vivo* studies involving nanocarriers are extremely complex which makes analyzing their toxicity to the different parts of the body complicated.<sup>255</sup> Nanocarriers are readily taken up by the living cells. However, the intracellular reactions and pathways of nanocarriers are not yet fully understood.<sup>256</sup> In addition, nanocarriers vary in their materials, shape, sizes, surface, charge, coating, matrix, dispersion agglomeration, and aggregation. Thus, different nanocarriers will have different reactions and toxicity levels. Therefore, their toxicity cannot be measured unless the nanocarriers are fully characterized.<sup>18</sup> Generally, the smaller the size of nanocarriers, the higher the toxicity.<sup>257</sup> Changing the shape of gold nanocarriers for example from spherical to the rod shape increased their toxicity.<sup>258</sup> In addition, nanocarriers with a positively charged surface are more toxic than negatively charged nanocarriers, the presence of a coating layer or a shell will result in a significant reduction in nanocarriers' toxicity.<sup>259</sup> Furthermore, while circulating in the blood, some of the nanocarriers may accumulate in specific organs of the body, resulting in toxic effects.<sup>260</sup> Despite these safety concerns, the research of developing nanocarrier technology promises to overcome these challenges and provide effective and safe cancer treatments.

## Conclusions

This paper reviews the growing technology of combining ultrasound with different nanocarriers to treat cancer. We have reported studies outlining the efficacy of ultrasound-responsive nanocarriers in *in vitro* and *in vivo* studies. However, several obstacles need to be addressed to ensure the success of ultrasound-responsive nanocarriers in clinical settings. More studies are needed to closely monitor the biodistribution and pharmacokinetics of ultrasound-responsive nanocarriers when ultrasound is applied *in vivo*. There is a need for continuous technological improvements to develop more biocompatible and effective ultrasound-responsive nanocarriers. Both the ultrasound parameters and nanocarrier specifications need to be optimized to ensure their successful use *in vitro*, *in vivo*, and future clinical trials.

## Conflicts of interest

There are no conflicts to declare.

## Acknowledgments

The authors would like to acknowledge funding from AUS Faculty Research Grants, Patient's Friends Committee-Sharjah, AlJalila Foundation, Al Qasimi Foundation, the Technology Innovation Pioneer-Healthcare Program, the Takamul program, and the Dana Gas Endowed Chair for Chemical Engineering.

## References

1. Cancer Research UK. Worldwide cancer statistics. <https://www.cancerresearchuk.org/health-professional/cancer-statistics/worldwide-cancer>. Accessed September 8, 2020.
2. Kaplun AP, Bezrukov DA, Shvets VI. Rational design of nano- and micro-size medicinal forms of biologically active substances. *Appl Biochem Microbiol*. 2011;47(8):711-717. doi:10.1134/s0003683811080072
3. Zhang L, Gu FX, Chan JM, Wang AZ, Langer RS, Farokhzad OC. Nanoparticles in Medicine: Therapeutic Applications and Developments. *Clin Pharmacol Ther*. 2007;83(5):761-769. doi:10.1038/sj.clpt.6100400
4. Din FU, Aman W, Ullah I, et al. Effective use of nanocarriers as drug delivery systems for the treatment of selected tumors. *Int J Nanomedicine*. 2017;12:7291-7309. doi:10.2147/IJN.S146315
5. Mishra B, Patel BB, Tiwari S. Colloidal nanocarriers: a review on formulation technology, types and applications toward targeted drug delivery. *Nanomedicine Nanotechnology, Biol Med*. 2010;6(1):9-24. doi:10.1016/j.nano.2009.04.008
6. Turk MJ, Reddy JA, Chmielewski JA, Low PS. Characterization of a novel pH-sensitive peptide that enhances drug release from folate-targeted liposomes at endosomal pHs. *Biochim Biophys Acta - Biomembr*. 2002;1559(1):56-68. doi:10.1016/s0005-2736(01)00441-2
7. O'Brien DF, Whitesides TH, Klingbiel RT. The

- photopolymerization of lipid-diacetylenes in bimolecular-layer membranes. *J Polym Sci Polym Lett Ed*. 1981;19(3):95-101. doi:10.1002/pol.1981.130190302
8. Zhu L, Kate P, Torchilin VP. Matrix Metalloprotease 2-Responsive Multifunctional Liposomal Nanocarrier for Enhanced Tumor Targeting. *ACS Nano*. 2012;6(4):3491-3498. doi:10.1021/nn300524f
9. Needham D, Anyarambhatla G, Kong G, Dewhirst MW. A New Temperature-sensitive Liposome for Use with Mild Hyperthermia: Characterization and Testing in a Human Tumor Xenograft Model. *Cancer Res*. 2000;60(5).
10. Pitt WG, Hussein GA, Staples BJ. Ultrasonic drug delivery – a general review. *Expert Opin Drug Deliv*. 2004;1(1):37-56. doi:10.1517/17425247.1.1.37
11. Hernot S, Klibanov AL. Microbubbles in ultrasound-triggered drug and gene delivery. *Adv Drug Deliv Rev*. 2008;60(10):1153-1166. doi:10.1016/j.addr.2008.03.005
12. Alexis F, Pridgen E, Molnar LK, Farokhzad OC. Factors Affecting the Clearance and Biodistribution of Polymeric Nanoparticles. *Mol Pharm*. 2008;5(4):505-515. doi:10.1021/mp800051m
13. Soo Choi H, Liu W, Misra P, et al. Renal clearance of quantum dots. *Nat Biotechnol*. 2007;25(10):1165-1170. doi:10.1038/nbt1340
14. Moghimi SM, Hedeman H, Muir IS, Illum L, Davis SS. An investigation of the filtration capacity and the fate of large filtered sterically-stabilized microspheres in rat spleen. *Biochim Biophys Acta - Gen Subj*. 1993;1157(2):233-240. doi:10.1016/0304-4165(93)90105-h
15. Mitragotri S, Anselmo AC. BioTM Buzz (Volume 5, Issue 3): The Future is Bright. *Bioeng Transl Med*. 2020. doi:10.1002/btm2.10185
16. Cavadas M, González-Fernández Á, Franco R. Pathogen-mimetic stealth nanocarriers for drug delivery: a future possibility. *Nanomedicine Nanotechnology, Biol Med*. 2011;7(6):730-743. doi:10.1016/j.nano.2011.04.006
17. Davis ME, Chen Z, Shin DM. Nanoparticle therapeutics: an emerging treatment modality for cancer. *Nat Rev Drug Discov*. 2008;7(9):771-782. doi:10.1038/nrd2614
18. Hossen S, Hossain MK, Basher MK, Mia MNH, Rahman MT, Uddin MJ. Smart nanocarrier-based drug delivery systems for cancer therapy and toxicity studies: A review. *J Adv Res*. 2019;15:1-18. doi:10.1016/j.jare.2018.06.005
19. Maeda H, Tsukigawa K, Fang J. A Retrospective 30 Years After Discovery of the Enhanced Permeability and Retention Effect of Solid Tumors: Next-Generation Chemotherapeutics and Photodynamic Therapy-Problems, Solutions, and Prospects. *Microcirculation*. 2016;23(3):173-182. doi:10.1111/micc.12228
20. Hatakeyama H, Akita H, Harashima H. The polyethyleneglycol dilemma: advantage and disadvantage of PEGylation of liposomes for systemic genes and nucleic acids delivery to tumors. *Biol Pharm Bull*. 2013;36(6):892-899. doi:10.1248/bpb.b13-00059
21. Clemons TD, Singh R, Sorolla A, Chaudhari N, Hubbard A, Iyer KS. Distinction Between Active and Passive Targeting of Nanoparticles Dictate Their Overall Therapeutic Efficacy. *Langmuir*. 2018;34(50):15343-15349. doi:10.1021/acs.langmuir.8b02946
22. Petros RA, DeSimone JM. Strategies in the design of nanoparticles for therapeutic applications. *Nat Rev Drug Discov*. 2010;9(8):615-627. doi:10.1038/nrd2591
23. Ibsen S, Schutt, Esener. Microbubble-mediated ultrasound therapy: a review of its potential in cancer treatment. *Drug Des Devel Ther*. 2013;375. doi:10.2147/dddt.s31564
24. Hu Q, Katti PS, Gu Z. Enzyme-responsive nanomaterials for controlled drug delivery. *Nanoscale*. 2014;6(21):12273-12286. doi:10.1039/c4nr04249b
25. Sim T, Lim C, Hoang NH, Oh KT. Recent advance of pH-sensitive nanocarriers targeting solid tumors. *J Pharm Investig*. 2017;47(5):383-394. doi:10.1007/s40005-017-0349-1
26. Karimi M, Sahandi Zangabad P, Ghasemi A, et al. Temperature-Responsive Smart Nanocarriers for Delivery of Therapeutic Agents: Applications and Recent Advances. *ACS Appl Mater Interfaces*. 2016;8(33):21107-21133. doi:10.1021/acsami.6b00371
27. Wang Y, Deng Y, Luo H, et al. Light-Responsive Nanoparticles for Highly Efficient Cytoplasmic Delivery of Anticancer Agents. *ACS Nano*. 2017;11(12):12134-12144. doi:10.1021/acsnano.7b05214
28. Muzzalupo R, Tavano L. Advances on Magnetic Nanocarriers Based on Natural Polymers. *Curr Pharm Des*. 2016;22(22):3353-3363. doi:10.2174/1381612822666160209152214
29. Ahmed SE, Moussa HG, Martins AM, Al-Sayah MH, Hussein GA. Effect of pH, ultrasound frequency and power density on the release of calcein from stealth liposomes. *nano Online*. 2017. doi:10.1515/nano.0012.2015-0046
30. Hussein GA, Pitt WG. Ultrasonic-Activated Micellar Drug Delivery for Cancer Treatment. *J Pharm Sci*. 2009;98(3):795-811. doi:10.1002/jps.21444
31. Ter Haar G. Therapeutic applications of ultrasound. *Prog Biophys Mol Biol*. 2007;93(1-3):111-129.
32. Schroeder A, Kost J, Barenholz Y. Ultrasound, liposomes, and drug delivery: principles for using ultrasound to control the release of drugs from liposomes. *Chem Phys Lipids*. 2009;162(1-2):1-16. doi:10.1016/j.chemphyslip.2009.08.003
33. Dalecki D. Mechanical Bioeffects of Ultrasound. *Annu Rev Biomed Eng*. 2004;6(1):229-248. doi:10.1146/annurev.bioeng.6.040803.140126
34. Ahmadi F, McLoughlin I V, Chauhan S, ter-Haar G. Bio-effects and safety of low-intensity, low-frequency ultrasonic exposure. *Prog Biophys Mol Biol*. 2012;108(3):119-138. doi:10.1016/j.pbiomolbio.2012.01.004
35. Humphrey VF. Ultrasound and matter—Physical interactions. *Prog Biophys Mol Biol*. 2007;93(1-3):195-211.
36. Hussein GA, Pitt WG, Martins AM. Ultrasonically triggered drug delivery: Breaking the barrier. *Colloids Surfaces B Biointerfaces*. 2014;123:364-386. doi:10.1016/j.colsurfb.2014.07.051
37. Postema M, van Wamel A, Lancée CT, de Jong N. Ultrasound-induced encapsulated microbubble phenomena. *Ultrasound Med Biol*. 2004;30(6):827-840. doi:10.1016/j.ultrasmedbio.2004.02.010
38. Prentice P, Cuschieri A, Dholakia K, Prausnitz M, Campbell P. Membrane disruption by optically controlled microbubble cavitation. *Nat Phys*. 2005;1(2):107-110. doi:10.1038/nphys148
39. VanBavel E. Effects of shear stress on endothelial cells:

- Possible relevance for ultrasound applications. *Prog Biophys Mol Biol.* 2007;93(1-3):374-383. doi:10.1016/j.pbiomolbio.2006.07.017
40. Wu J. Theoretical study on shear stress generated by microstreaming surrounding contrast agents attached to living cells. *Ultrasound Med Biol.* 2002;28(1):125-129. doi:10.1016/s0301-5629(01)00497-5
41. Wu J. Shear stress in cells generated by ultrasound. *Prog Biophys Mol Biol.* 2007;93(1-3):363-373.
42. Lentacker I, De Cock I, Deckers R, De Smedt SC, Moonen CTW. Understanding ultrasound induced sonoporation: Definitions and underlying mechanisms. *Adv Drug Deliv Rev.* 2014;72:49-64. doi:10.1016/j.addr.2013.11.008
43. Qiu Y, Luo Y, Zhang Y, et al. The correlation between acoustic cavitation and sonoporation involved in ultrasound-mediated DNA transfection with polyethylenimine (PEI) in vitro. *J Control Release.* 2010;145(1):40-48. doi:10.1016/j.jconrel.2010.04.010
44. Yang F, Gu N, Chen D, et al. Experimental study on cell self-sealing during sonoporation. *J Control Release.* 2008;131(3):205-210. doi:10.1016/j.jconrel.2008.07.038
45. Riesz P, Berdahl D, Christman CL. Free radical generation by ultrasound in aqueous and nonaqueous solutions. *Environ Health Perspect.* 1985;64:233-252. doi:10.1289/ehp.8564233
46. Canavese G, Ancona A, Racca L, et al. Nanoparticle-assisted ultrasound: A special focus on sonodynamic therapy against cancer. *Chem Eng J.* 2018;340:155-172. doi:10.1016/j.cej.2018.01.060
47. Hilgenfeldt S, Grossmann S, Lohse D. A simple explanation of light emission in sonoluminescence. *Nature.* 1999;398(6726):402-405. doi:10.1038/18842
48. Costley D, Mc Ewan C, Fowley C, et al. Treating cancer with sonodynamic therapy: A review. *Int J Hypertherm.* 2015;31(2):107-117. doi:10.3109/02656736.2014.992484
49. Kondo T, Krishna CM, Riesz P. Free Radical Generation by Ultrasound in Aqueous Solutions of Nucleic Acid Bases and Nucleosides: An ESR and Spin-trapping Study. *Int J Radiat Biol.* 1988;53(2):331-342. doi:10.1080/09553008814550681
50. Halliwell B, Aruoma OI. DNA damage by oxygen-derived species Its mechanism and measurement in mammalian systems. *FEBS Lett.* 1991;281(1-2):9-19. doi:10.1016/0014-5793(91)80347-6
51. Honda H, Kondo T, Zhao Q-L, Feril LB, Kitagawa H. Role of intracellular calcium ions and reactive oxygen species in apoptosis induced by ultrasound. *Ultrasound Med Biol.* 2004;30(5):683-692. doi:10.1016/j.ultrasmedbio.2004.02.008
52. Furusawa Y, Hassan MA, Zhao Q-L, Ogawa R, Tabuchi Y, Kondo T. Effects of therapeutic ultrasound on the nucleus and genomic DNA. *Ultrason Sonochem.* 2014;21(6):2061-2068. doi:10.1016/j.ultsonch.2014.02.028
53. Afadzi M, Strand SP, Nilssen EA, et al. Mechanisms of the ultrasound-mediated intracellular delivery of liposomes and dextrans. *IEEE Trans Ultrason Ferroelectr Freq Control.* 2013;60(1). doi:10.1109/tuffc.2013.2534
54. Schlicher RK, Radhakrishna H, Tolentino TP, Apkarian RP, Zarnitsyn V, Prausnitz MR. Mechanism of intracellular delivery by acoustic cavitation. *Ultrasound Med Biol.* 2006;32(6):915-924. doi:10.1016/j.ultrasmedbio.2006.02.1416
55. Sato M, Nagata K, Kuroda S, et al. Low-Intensity Pulsed Ultrasound Activates Integrin-Mediated Mechanotransduction Pathway in Synovial Cells. *Ann Biomed Eng.* 2014;42(10):2156-2163. doi:10.1007/s10439-014-1081-x
56. Lionetti V, Fittipaldi A, Agostini S, Giacca M, Recchia FA, Picano E. Enhanced Caveolae-Mediated Endocytosis by Diagnostic Ultrasound In Vitro. *Ultrasound Med Biol.* 2009;35(1):136-143. doi:10.1016/j.ultrasmedbio.2008.07.011
57. Tardoski S, Gineyts E, Ngo J, Kocot A, Clézardin P, Melodelima D. Low-Intensity Ultrasound Promotes Clathrin-Dependent Endocytosis for Drug Penetration into Tumor Cells. *Ultrasound Med Biol.* 2015;41(10):2740-2754. doi:10.1016/j.ultrasmedbio.2015.06.006
58. Meijering BDM, Juffermans LJM, van Wamel A, et al. Ultrasound and microbubble-targeted delivery of macromolecules is regulated by induction of endocytosis and pore formation. *Circ Res.* 2009;104(5):679-687. doi:10.1161/CIRCRESAHA.108.183806
59. Shortencarier MJ, Dayton PA, Bloch SH, Schumann PA, Matsunaga TO, Ferrara KW. A method for radiation-force localized drug delivery using gas-filled lipospheres. *IEEE Trans Ultrason Ferroelectr Freq Control.* 2004;51(7):822-831. doi:10.1109/tuffc.2004.1320741
60. Hancock HA, Smith LH, Cuesta J, et al. Investigations into Pulsed High-Intensity Focused Ultrasound-Enhanced Delivery: Preliminary Evidence for a Novel Mechanism. *Ultrasound Med Biol.* 2009;35(10):1722-1736. doi:10.1016/j.ultrasmedbio.2009.04.020
61. van der Zee J. Heating the patient: a promising approach? *Ann Oncol.* 2002;13(8):1173-1184. doi:10.1093/annonc/mdf280
62. VanderWaal R, Malyapa RS, Higashikubo R, Roti JLR. A Comparison of the Modes and Kinetics of Heat-Induced Cell Killing in HeLa and L5178Y Cells. *Radiat Res.* 1997;148(5):455. doi:10.2307/3579323
63. Konings AWT, Ruifrok ACC. Role of Membrane Lipids and Membrane Fluidity in Thermosensitivity and Thermotolerance of Mammalian Cells. *Radiat Res.* 1985;102(1):86. doi:10.2307/3576432
64. Coss RA, Linnemans WAM. The effects of hyperthermia on the cytoskeleton: a review. *Int J Hypertherm.* 1996;12(2):173-196. doi:10.3109/02656739609022507
65. Oyama K, Arai T, Isaka A, et al. Directional Bleb Formation in Spherical Cells under Temperature Gradient. *Biophys J.* 2015;109(2):355-364. doi:10.1016/j.bpj.2015.06.016
66. Kapiszewska M, Hopwood LE. Changes in Bleb Formation Following Hyperthermia Treatment of Chinese Hamster Ovary Cells. *Radiat Res.* 1986;105(3):405. doi:10.2307/3576695
67. Majda JA, Gerner EW, Vanlandingham B, Gehlsen KR, Cress AE. Heat Shock-Induced Shedding of Cell Surface Integrins in A549 Human Lung Tumor Cells in Culture. *Exp Cell Res.* 1994;210(1):46-51. doi:10.1006/excr.1994.1007
68. Lepock JR. Cellular effects of hyperthermia: relevance to the minimum dose for thermal damage. *Int J Hypertherm.* 2003;19(3):252-266. doi:10.1080/0265673031000065042
69. Speed CA. Therapeutic ultrasound in soft tissue lesions. *Rheumatology.* 2001;40(12):1331-1336.

- doi:10.1093/rheumatology/40.12.1331
70. Rosenthal I, Sostaric JZ, Riesz P. Enlightened sonochemistry. *Res Chem Intermed*. 2004;30(7-8):685-701. doi:10.1163/1568567041856936
71. Shibaguchi H, Tsuru H, Kuroki M, Kuroki M. Enhancement of the Antitumor Effect on Combination Therapy of an Anticancer Drug and Its Antibody against Carcinoembryonic Antigen. *Chemotherapy*. 2012;58(2):110-117. doi:10.1159/000337068
72. Lodeiro C, Capelo-Martnez J-L. Beyond Analytical Chemistry. *Ultrasound Chem*.:129-150. doi:10.1002/9783527623501.ch6
73. Kennedy JE. High-intensity focused ultrasound in the treatment of solid tumours. *Nat Rev Cancer*. 2005;5(4):321-327. doi:10.1038/nrc1591
74. Guan L, Xu G. Damage effect of high-intensity focused ultrasound on breast cancer tissues and their vascularities. *World J Surg Oncol*. 2016;14(1). doi:10.1186/s12957-016-0908-3
75. Jung Y, Reif R, Zeng Y, Wang RK. Three-Dimensional High-Resolution Imaging of Gold Nanorods Uptake in Sentinel Lymph Nodes. *Nano Lett*. 2011;11(7):2938-2943. doi:10.1021/nl2014394
76. Hu Z, Yang XY, Liu Y, et al. Release of endogenous danger signals from HIFU-treated tumor cells and their stimulatory effects on APCs. *Biochem Biophys Res Commun*. 2005;335(1):124-131. doi:10.1016/j.bbrc.2005.07.071
77. Xu H, Zhang X, Han R, et al. Nanoparticles in sonodynamic therapy: state of the art review. *RSC Adv*. 2016;6(56):50697-50705. doi:10.1039/c6ra06862f
78. Trendowski M. The promise of sonodynamic therapy. *Cancer Metastasis Rev*. 2013;33(1):143-160. doi:10.1007/s10555-013-9461-5
79. Pang X, Xu C, Jiang Y, Xiao Q, Leung AW. Natural products in the discovery of novel sonosensitizers. *Pharmacol Ther*. 2016;162:144-151. doi:10.1016/j.pharmthera.2015.12.004
80. Escoffre JM, Piron J, Novell A, Bouakaz A. Doxorubicin Delivery into Tumor Cells with Ultrasound and Microbubbles. *Mol Pharm*. 2011;8(3):799-806. doi:10.1021/mp100397p
81. Wu J, Pepe J, Rincón M. Sonoporation, anti-cancer drug and antibody delivery using ultrasound. *Ultrasonics*. 2006;44:e21-e25. doi:10.1016/j.ultras.2006.06.033
82. Huber PE, Pfisterer P. In vitro and in vivo transfection of plasmid DNA in the Dunning prostate tumor R3327-AT1 is enhanced by focused ultrasound. *Gene Ther*. 2000;7(17):1516-1525. doi:10.1038/sj.gt.3301242
83. van Wamel A, Bouakaz A, Versluis M, de Jong N. Micromanipulation of endothelial cells: Ultrasound-microbubble-cell interaction. *Ultrasound Med Biol*. 2004;30(9):1255-1258. doi:10.1016/j.ultrasmedbio.2004.07.015
84. Mura S, Nicolas J, Couvreur P. Stimuli-responsive nanocarriers for drug delivery. *Nat Mater*. 2013;12(11):991-1003. doi:10.1038/nmat3776
85. Zanelli CI, DeMarta S, Hennige CW, Kadri MM. Beamforming for therapy with high intensity focused ultrasound (HIFU) using quantitative schlieren. *1993 Proc IEEE Ultrason Symp*. 1993. doi:10.1109/ultsym.1993.339610
86. Ibsen S, Benchimol M, Simberg D, Schutt C, Steiner J, Esener S. A novel nested liposome drug delivery vehicle capable of ultrasound triggered release of its payload. *J Control Release*. 2011;155(3):358-366. doi:10.1016/j.jconrel.2011.06.032
87. Kheirilomoom A, Mahakian LM, Lai C-Y, et al. Copper-Doxorubicin as a Nanoparticle Cargo Retains Efficacy with Minimal Toxicity. *Mol Pharm*. 2010;7(6):1948-1958. doi:10.1021/mp100245u
88. Wan G-Y, Wan G-Y, Liu Y, et al. Recent advances of sonodynamic therapy in cancer treatment. *Cancer Biol Med*. 2016;13(3):325-338. doi:10.20892/j.issn.2095-3941.2016.0068
89. Wang Y, Zhao Q, Han N, et al. Mesoporous silica nanoparticles in drug delivery and biomedical applications. *Nanomedicine Nanotechnology, Biol Med*. 2015;11(2):313-327. doi:10.1016/j.nano.2014.09.014
90. Lu J, Liong M, Li Z, Zink JJ, Tamanoi F. Biocompatibility, Biodistribution, and Drug-Delivery Efficiency of Mesoporous Silica Nanoparticles for Cancer Therapy in Animals. *Small*. 2010;6(16):1794-1805. doi:10.1002/smll.201000538
91. Manzano M, Vallet-Regí M. Ultrasound responsive mesoporous silica nanoparticles for biomedical applications. *Chem Commun*. 2019;55(19):2731-2740. doi:10.1039/c8cc09389j
92. Horcajada P, Rámila A, Pérez-Pariente J, Vallet-Regí M. Influence of pore size of MCM-41 matrices on drug delivery rate. *Microporous Mesoporous Mater*. 2004;68(1-3):105-109. doi:10.1016/j.micromeso.2003.12.012
93. Vallet-Regí M. Ordered Mesoporous Materials in the Context of Drug Delivery Systems and Bone Tissue Engineering. *Chem - A Eur J*. 2006;12(23):5934-5943. doi:10.1002/chem.200600226
94. Paris JL, Cabañas MV, Manzano M, Vallet-Regí M. Polymer-Grafted Mesoporous Silica Nanoparticles as Ultrasound-Responsive Drug Carriers. *ACS Nano*. 2015;9(11):11023-11033. doi:10.1021/acsnano.5b04378
95. Paris JL, Manzano M, Cabañas MV, Vallet-Regí M. Mesoporous silica nanoparticles engineered for ultrasound-induced uptake by cancer cells. *Nanoscale*. 2018;10(14):6402-6408. doi:10.1039/c8nr00693h
96. Li X, Wang Z, Xia H. Ultrasound Reversible Response Nanocarrier Based on Sodium Alginate Modified Mesoporous Silica Nanoparticles. *Front Chem*. 2019;7. doi:10.3389/fchem.2019.00059
97. Wang J, Jiao Y, Shao Y. Mesoporous Silica Nanoparticles for Dual-Mode Chemo-Sonodynamic Therapy by Low-Energy Ultrasound. *Materials (Basel)*. 2018;11(10):2041. doi:10.3390/ma11102041
98. Sviridov AP, Osminkina LA, Nikolaev AL, Kudryavtsev AA, Vasiliev AN, Timoshenko VY. Lowering of the cavitation threshold in aqueous suspensions of porous silicon nanoparticles for sonodynamic therapy applications. *Appl Phys Lett*. 2015;107(12):123107. doi:10.1063/1.4931728
99. Zhao Y, Zhu Y. Synergistic cytotoxicity of low-energy ultrasound and innovative mesoporous silica-based sensitive nanoagents. *J Mater Sci*. 2014;49(10):3665-3673. doi:10.1007/s10853-014-8073-y
100. Osminkina LA, Gongalsky MB, Motuzuk A V, Timoshenko VY, Kudryavtsev AA. Silicon nanocrystals as photo- and sono-sensitizers for biomedical applications. *Appl Phys B*.

- 2011;105(3):665-668. doi:10.1007/s00340-011-4562-8
101. Revia RA, Zhang M. Magnetite nanoparticles for cancer diagnosis, treatment, and treatment monitoring: recent advances. *Mater Today*. 2016;19(3):157-168. doi:10.1016/j.mattod.2015.08.022
102. Zhao X, Milton Harris J. Novel Degradable Poly(Ethylene Glycol) Hydrogels for Controlled Release of Protein. *J Pharm Sci*. 1998;87(11):1450-1458. doi:10.1021/js980065o
103. Tartaj P, Serna CJ. Synthesis of Monodisperse Superparamagnetic Fe/Silica Nanospherical Composites. *J Am Chem Soc*. 2003;125(51):15754-15755. doi:10.1021/ja0380594
104. Mahmoudi M, Sant S, Wang B, Laurent S, Sen T. Superparamagnetic iron oxide nanoparticles (SPIONs): Development, surface modification and applications in chemotherapy. *Adv Drug Deliv Rev*. 2011;63(1-2):24-46. doi:10.1016/j.addr.2010.05.006
105. Yiu HHP, Pickard MR, Olariu CI, Williams SR, Chari DM, Rosseinsky MJ. Fe<sub>3</sub>O<sub>4</sub>-PEI-RITC Magnetic Nanoparticles with Imaging and Gene Transfer Capability: Development of a Tool for Neural Cell Transplantation Therapies. *Pharm Res*. 2011;29(5):1328-1343. doi:10.1007/s11095-011-0632-1
106. Paik S-Y-R, Kim J-S, Shin S, Ko S. Characterization, Quantification, and Determination of the Toxicity of Iron Oxide Nanoparticles to the Bone Marrow Cells. *Int J Mol Sci*. 2015;16(9):22243-22257. doi:10.3390/ijms160922243
107. Couto D, Sousa R, Andrade L, et al. Polyacrylic acid coated and non-coated iron oxide nanoparticles are not genotoxic to human T lymphocytes. *Toxicol Lett*. 2015;234(2):67-73. doi:10.1016/j.toxlet.2015.02.010
108. Bourrinet P, Bengel HH, Bonnemain B, et al. Preclinical Safety and Pharmacokinetic Profile of Ferumoxtran-10, an Ultrasmall Superparamagnetic Iron Oxide Magnetic Resonance Contrast Agent. *Invest Radiol*. 2006;41(3):313-324. doi:10.1097/01.rli.0000197669.80475.dd
109. Chamorro S, Gutiérrez L, Vaquero MP, et al. Safety assessment of chronic oral exposure to iron oxide nanoparticles. *Nanotechnology*. 2015;26(20):205101. doi:10.1088/0957-4484/26/20/205101
110. Yang X, Ma, Luo, et al. Intraperitoneal injection of magnetic Fe<sub>3</sub>O<sub>4</sub>-nanoparticle induces hepatic and renal tissue injury via oxidative stress in mice. *Int J Nanomedicine*. 2012;4809. doi:10.2147/ijn.s34349
111. Wu W, He Q, Jiang C. Magnetic Iron Oxide Nanoparticles: Synthesis and Surface Functionalization Strategies. *Nanoscale Res Lett*. 2008;3(11):397-415. doi:10.1007/s11671-008-9174-9
112. Lin Z, Monteiro-Riviere NA, Riviere JE. Pharmacokinetics of metallic nanoparticles. *Wiley Interdiscip Rev Nanomedicine Nanobiotechnology*. 2014;7(2):189-217. doi:10.1002/wnan.1304
113. Ebrahimi Fard A, Zarepour A, Zarrabi A, Shanei A, Salehi H. Synergistic effect of the combination of triethylene-glycol modified Fe<sub>3</sub>O<sub>4</sub> nanoparticles and ultrasound wave on MCF-7 cells. *J Magn Magn Mater*. 2015;394:44-49. doi:10.1016/j.jmmm.2015.06.040
114. Ninomiya K, Noda K, Ogino C, Kuroda S, Shimizu N. Enhanced OH radical generation by dual-frequency ultrasound with TiO<sub>2</sub> nanoparticles: Its application to targeted sonodynamic therapy. *Ultrason Sonochem*. 2014;21(1):289-294. doi:10.1016/j.ultsonch.2013.05.005
115. Shen Y, Pi Z, Yan F, et al. Enhanced delivery of paclitaxel liposomes using focused ultrasound with microbubbles for treating nude mice bearing intracranial glioblastoma xenografts. *Int J Nanomedicine*. 2017;Volume 12:5613-5629. doi:10.2147/ijn.s136401
116. Zavaleta CL, Smith BR, Walton I, et al. Multiplexed imaging of surface enhanced Raman scattering nanotags in living mice using noninvasive Raman spectroscopy. *Proc Natl Acad Sci*. 2009;106(32):13511-13516. doi:10.1073/pnas.0813327106
117. Kim D, Jeong YY, Jon S. A Drug-Loaded Aptamer-Gold Nanoparticle Bioconjugate for Combined CT Imaging and Therapy of Prostate Cancer. *ACS Nano*. 2010;4(7):3689-3696. doi:10.1021/nn901877h
118. Dreaden EC, Austin LA, Mackey MA, El-Sayed MA. Size matters: gold nanoparticles in targeted cancer drug delivery. *Ther Deliv*. 2012;3(4):457-478. doi:10.4155/tde.12.21
119. Chithrani BD, Chan WCW. Elucidating the Mechanism of Cellular Uptake and Removal of Protein-Coated Gold Nanoparticles of Different Sizes and Shapes. *Nano Lett*. 2007;7(6):1542-1550. doi:10.1021/nl070363y
120. Dykman LA, Khlebtsov NG. Gold Nanoparticles in Biology and Medicine: Recent Advances and Prospects. *Acta Naturae*. 2011;3(2):34-55. doi:10.32607/20758251-2011-3-2-34-55
121. Yang P-H, Sun X, Chiu J-F, Sun H, He Q-Y. Transferrin-Mediated Gold Nanoparticle Cellular Uptake. *Bioconjug Chem*. 2005;16(3):494-496. doi:10.1021/bc049775d
122. Han G, Ghosh P, De M, Rotello VM. Drug and gene delivery using gold nanoparticles. *NanoBiotechnology*. 2007;3(1):40-45. doi:10.1007/s12030-007-0005-3
123. Deng CX, Xu Q, Apfel RE, Holland CK. Inertial cavitation produced by pulsed ultrasound in controlled host media. *J Acoust Soc Am*. 1996;100(2):1199-1208. doi:10.1121/1.416304
124. Brazzale C, Canaparo R, Racca L, et al. Enhanced selective sonosensitizing efficacy of ultrasound-based anticancer treatment by targeted gold nanoparticles. *Nanomedicine*. 2016;11(23):3053-3070. doi:10.2217/nnm-2016-0293
125. Kosheleva OK, Lai T-C, Chen NG, Hsiao M, Chen C-H. Selective killing of cancer cells by nanoparticle-assisted ultrasound. *J Nanobiotechnology*. 2016;14(1). doi:10.1186/s12951-016-0194-9
126. Sazgarnia A, Shanei A, Taheri AR, et al. Therapeutic Effects of Acoustic Cavitation in the Presence of Gold Nanoparticles on a Colon Tumor Model. *J Ultrasound Med*. 2013;32(3):475-483. doi:10.7863/jum.2013.32.3.475
127. Shanei A, Sazgarnia A, Tayyebi Meibodi N, et al. Sonodynamic Therapy Using Protoporphyrin IX Conjugated to Gold Nanoparticles: An In Vivo Study on a Colon Tumor Model. *Iran J Basic Med Sci*. 2012;15(2):759-767. <http://www.ncbi.nlm.nih.gov/pubmed/23493546>. Accessed September 7, 2020.
128. Mehra NK, Mishra V, Jain NK. A review of ligand tethered surface engineered carbon nanotubes. *Biomaterials*. 2014;35(4):1267-1283. doi:10.1016/j.biomaterials.2013.10.032
129. Sanginario A, Miccoli B, Demarchi D. Carbon Nanotubes as an Effective Opportunity for Cancer Diagnosis and

- Treatment. *Biosensors*. 2017;7(4):9. doi:10.3390/bios7010009
130. Raval JP, Joshi P, Chejara DR. Carbon nanotube for targeted drug delivery. *Appl Nanocomposite Mater Drug Deliv*. 2018;203-216. doi:10.1016/b978-0-12-813741-3.00009-1
131. Mahajan S, Patharkar A, Kuche K, et al. Functionalized carbon nanotubes as emerging delivery system for the treatment of cancer. *Int J Pharm*. 2018;548(1):540-558. doi:10.1016/j.ijpharm.2018.07.027
132. Hashida Y, Tanaka H, Zhou S, et al. Photothermal ablation of tumor cells using a single-walled carbon nanotube-peptide composite. *J Control Release*. 2014;173:59-66. doi:10.1016/j.jconrel.2013.10.039
133. Shi J, Ma R, Wang L, et al. The application of hyaluronic acid-derivatized carbon nanotubes in hematoporphyrin monomethyl ether-based photodynamic therapy for in vivo and in vitro cancer treatment. *Int J Nanomedicine*. 2013;2361. doi:10.2147/ijn.s45407
134. Gu F, Hu C, Xia Q, Gong C, Gao S, Chen Z. Aptamer-conjugated multi-walled carbon nanotubes as a new targeted ultrasound contrast agent for the diagnosis of prostate cancer. *J Nanoparticle Res*. 2018;20(11). doi:10.1007/s11051-018-4407-z
135. Wu H, Shi H, Zhang H, et al. Prostate stem cell antigen antibody-conjugated multiwalled carbon nanotubes for targeted ultrasound imaging and drug delivery. *Biomaterials*. 2014;35(20):5369-5380. doi:10.1016/j.biomaterials.2014.03.038
136. Delogu LG, Vidili G, Venturelli E, et al. Functionalized multiwalled carbon nanotubes as ultrasound contrast agents. *Proc Natl Acad Sci*. 2012;109(41):16612-16617. doi:10.1073/pnas.1208312109
137. Pagani G, Green MJ, Poulin P, Pasquali M. Competing mechanisms and scaling laws for carbon nanotube scission by ultrasonication. *Proc Natl Acad Sci*. 2012;109(29):11599-11604. doi:10.1073/pnas.1200013109
138. Arrigo R, Teresi R, Gambarotti C, Parisi F, Lazzara G, Dintcheva N. Sonication-Induced Modification of Carbon Nanotubes: Effect on the Rheological and Thermo-Oxidative Behaviour of Polymer-Based Nanocomposites. *Materials (Basel)*. 2018;11(3):383. doi:10.3390/ma11030383
139. Sesis A, Hodnett M, Memoli G, et al. Influence of Acoustic Cavitation on the Controlled Ultrasonic Dispersion of Carbon Nanotubes. *J Phys Chem B*. 2013;117(48):15141-15150. doi:10.1021/jp410041y
140. Ruan B, Jacobi AM. Ultrasonication effects on thermal and rheological properties of carbon nanotube suspensions. *Nanoscale Res Lett*. 2012;7(1). doi:10.1186/1556-276x-7-127
141. Hansen SF, Lennquist A. SIN List criticism based on misunderstandings. *Nat Nanotechnol*. 2020;15(6):418. doi:10.1038/s41565-020-0692-7
142. Sutton D, Nasongkla N, Blanco E, Gao J. Functionalized Micellar Systems for Cancer Targeted Drug Delivery. *Pharm Res*. 2007;24(6):1029-1046. doi:10.1007/s11095-006-9223-y
143. Zhou Q, Zhang L, Yang T, Wu H. Stimuli-responsive polymeric micelles for drug delivery and cancer therapy. *Int J Nanomedicine*. 2018;Volume 13:2921-2942. doi:10.2147/ijn.s158696
144. Ahmed SE, Awad N, Paul V, Moussa HG, Hussein GA. Improving the Efficacy of Anticancer Drugs via Encapsulation and Acoustic Release. *Curr Top Med Chem*. 2018;18(10):857-880. doi:10.2174/1568026618666180608125344
145. Hussein GA, Pitt WG. Micelles and nanoparticles for ultrasonic drug and gene delivery. *Adv Drug Deliv Rev*. 2008;60(10):1137-1152. doi:10.1016/j.addr.2008.03.008
146. Hussein GA, Velluto D, Kherbeck L, Pitt WG, Hubbell JA, Christensen DA. Investigating the acoustic release of doxorubicin from targeted micelles. *Colloids Surfaces B Biointerfaces*. 2013;101:153-155. doi:10.1016/j.colsurfb.2012.05.025
147. Pitt WG, Hussein GA, Kherbeck LN. CHAPTER 6. Ultrasound-triggered Release from Micelles. *Smart Mater Ser*.:148-178. doi:10.1039/9781849736800-00148
148. Salgarella AR, Zahoranová A, Šrámková P, et al. Investigation of drug release modulation from poly(2-oxazoline) micelles through ultrasound. *Sci Rep*. 2018;8(1). doi:10.1038/s41598-018-28140-3
149. Xuan J, Boissière O, Zhao Y, et al. Ultrasound-Responsive Block Copolymer Micelles Based on a New Amplification Mechanism. *Langmuir*. 2012;28(47):16463-16468. doi:10.1021/la303946b
150. Wu P, Jia Y, Qu F, et al. Ultrasound-Responsive Polymeric Micelles for Sonoporation-Assisted Site-Specific Therapeutic Action. *ACS Appl Mater Interfaces*. 2017;9(31):25706-25716. doi:10.1021/acsami.7b05469
151. Liang B, Tong R, Wang Z, Guo S, Xia H. High Intensity Focused Ultrasound Responsive Metallo-supramolecular Block Copolymer Micelles. *Langmuir*. 2014;30(31):9524-9532. doi:10.1021/la500841x
152. Staples BJ, Roeder BL, Hussein GA, Badamjav O, Schaalje GB, Pitt WG. Role of frequency and mechanical index in ultrasonic-enhanced chemotherapy in rats. *Cancer Chemother Pharmacol*. 2009;64(3):593-600. doi:10.1007/s00280-008-0910-8
153. Hasanzadeh H, Mokhtari-Dizaji M, Zahra Bathaie S, Hassan ZM. Effect of local dual frequency sonication on drug distribution from polymeric nanomicelles. *Ultrason Sonochem*. 2011;18(5):1165-1171. doi:10.1016/j.ultsonch.2011.03.018
154. Rapoport N. Combined cancer therapy by micellar-encapsulated drug and ultrasound. *Int J Pharm*. 2004;277(1-2):155-162.
155. Nelson JL, Roeder BL, Carmen JC, Roloff F, Pitt WG. Ultrasonically activated chemotherapeutic drug delivery in a rat model. *Cancer Res*. 2002;62(24):7280-7283.
156. Hussein GA, Myrup GD, Pitt WG, Christensen DA, Rapoport NY. Factors affecting acoustically triggered release of drugs from polymeric micelles. *J Control Release*. 2000;69(1):43-52. doi:10.1016/s0168-3659(00)00278-9
157. Munshi N, Rapoport N, Pitt WG. Ultrasonic activated drug delivery from Pluronic P-105 micelles. *Cancer Lett*. 1997;118(1):13-19. doi:10.1016/s0304-3835(97)00218-8
158. Zeng Y, Pitt WG. A polymeric micelle system with a hydrolysable segment for drug delivery. *J Biomater Sci Polym Ed*. 2006;17(5):591-604. doi:10.1163/156856206776986297
159. Marin A, Sun H, Hussein GA, Pitt WG, Christensen DA, Rapoport NY. Drug delivery in pluronic micelles: Effect of

- high-frequency ultrasound on drug release from micelles and intracellular uptake. *J Control Release*. 2002;84(1-2):39-47. doi:10.1016/S0168-3659(02)00262-6
160. Marin A, Muniruzzaman M, Rapoport N. Acoustic activation of drug delivery from polymeric micelles: effect of pulsed ultrasound. *J Control Release*. 2001;71(3):239-249. doi:10.1016/s0168-3659(01)00216-4
161. Gao Z-G, Fain HD, Rapoport N. Controlled and targeted tumor chemotherapy by micellar-encapsulated drug and ultrasound. *J Control Release*. 2005;102(1):203-222.
162. Hussein GA, Diaz De La Rosa MA, Richardson ES, Christensen DA, Pitt WG. The role of cavitation in acoustically activated drug delivery. *J Control Release*. 2005;107(2):253-261. doi:10.1016/j.jconrel.2005.06.015
163. Hussein GA, O'Neill KL, Pitt WG. The comet assay to determine the mode of cell death for the ultrasonic delivery of doxorubicin to human leukemia (HL-60 Cells) from Pluronic P105 micelles. *Technol Cancer Res Treat*. 2005;4(6):707-711.
164. Zhang H, Xia H, Wang J, Li Y. High intensity focused ultrasound-responsive release behavior of PLA-b-PEG copolymer micelles. *J Control Release*. 2009;139(1):31-39. doi:10.1016/j.jconrel.2009.05.037
165. Hussein GA, El-Fayoumi RI, O'Neill KL, Rapoport NY, Pitt WG. DNA damage induced by micellar-delivered doxorubicin and ultrasound: comet assay study. *Cancer Lett*. 2000;154(2):211-216.
166. Hussein GA, Rapoport NY, Christensen DA, Pruitt JD, Pitt WG. Kinetics of ultrasonic release of doxorubicin from pluronic P105 micelles. *Colloids Surfaces B Biointerfaces*. 2002;24(3-4):253-264. doi:10.1016/S0927-7765(01)00273-9
167. Hussein GA, Runyan CM, Pitt WG. Investigating the mechanism of acoustically activated uptake of drugs from Pluronic micelles. *BMC Cancer*. 2002;2(1):1-6.
168. Hussein GA, Kherbeck L, Pitt WG, Hubbell JA, Christensen DA, Velluto D. Kinetics of ultrasonic drug delivery from targeted micelles. *J Nanosci Nanotechnol*. 2015;15(3):2099-2104. doi:10.1166/jnn.2015.9498
169. Tong R, Xia H, Lu X. Fast release behavior of block copolymer micelles under high intensity focused ultrasound/redox combined stimulus. *J Mater Chem B*. 2013;1(6):886-894. doi:10.1039/c2tb00222a
170. Hussein GA, Diaz de la Rosa MA, Gabuji T, Zeng Y, Christensen DA, Pitt WG. Release of doxorubicin from unstabilized and stabilized micelles under the action of ultrasound. *J Nanosci Nanotechnol*. 2007;7(3):1028-1033. doi:10.1166/jnn.2007.218
171. Yoshina-Ishii C, Miller GP, Kraft ML, Kool ET, Boxer SG. General method for modification of liposomes for encoded assembly on supported bilayers. *J Am Chem Soc*. 2005;127(5):1356-1357.
172. Papahadjopoulos D, Allen TM, Gabizon A, et al. Sterically stabilized liposomes: Improvements in pharmacokinetics and antitumor therapeutic efficacy. *Proc Natl Acad Sci U S A*. 1991;88(24):11460-11464. doi:10.1073/pnas.88.24.11460
173. Mayer LD, Nayar R, Thies RL, Boman NL, Cullis PR, Bally MB. Identification of vesicle properties that enhance the antitumor activity of liposomal vincristine against murine L1210 leukemia. *Cancer Chemother Pharmacol*. 1993;33(1):17-24.
174. Boman NL, Bally MB, Cullis PR, Mayer LD, Webb MS. Encapsulation of vincristine in liposomes reduces its toxicity and improves its anti-tumor efficacy. *J Liposome Res*. 1995;5(3):523-541.
175. Allen TM, Cullis PR. Liposomal drug delivery systems: From concept to clinical applications. *Adv Drug Deliv Rev*. 2013;65(1):36-48. doi:10.1016/j.addr.2012.09.037
176. Barenholz Y. Doxil®--the first FDA-approved nano-drug: lessons learned. *J Control Release*. 2012;160(2):117-134. doi:10.1016/j.jconrel.2012.03.020
177. Hussein G, Abbas Y, Awad N. The Potential of Ultrasound Technology and Chemotherapy Carriers in Breast Cancer Treatment. *Al Qasimi Found*. May 2018. doi:10.18502/aqf.0059
178. Maeda H, Wu J, Sawa T, Matsumura Y, Hori K. Maeda H, Wu J, Sawa T, Matsumura Y, Hori K. Tumor vascular permeability and the EPR effect in macromolecular therapeutics: a review. *J Control Rel* 65: 271-284. *J Control Release*. 2000;65:271-284. doi:10.1016/S0168-3659(99)00248-5
179. Cheong I, Huang X, Bettegowda C, et al. A bacterial protein enhances the release and efficacy of liposomal cancer drugs. *Science*. 2006;314(5803):1308-1311. doi:10.1126/science.1130651
180. Yu T, Wang Z, Mason TJ. A review of research into the uses of low level ultrasound in cancer therapy. *Ultrason Sonochem*. 2004;11(2):95-103. doi:10.1016/S1350-4177(03)00157-3
181. Lin HY, Thomas JL. PEG-lipids and oligo (ethylene glycol) surfactants enhance the ultrasonic permeabilizability of liposomes. *Langmuir*. 2003;19(4):1098-1105. doi:10.1021/la026604t
182. Evjen TJ, Nilssen EA, Røgnvaldsson S, Brandl M, Fossheim SL. Distearoylphosphatidylethanolamine-based liposomes for ultrasound-mediated drug delivery. *Eur J Pharm Biopharm*. 2010;75(3):327-333. doi:10.1016/j.ejpb.2010.04.012
183. Evjen TJ, Hupfeld S, Barnert S, Fossheim S, Schubert R, Brandl M. Physicochemical characterization of liposomes after ultrasound exposure - mechanisms of drug release. *J Pharm Biomed Anal*. 2013;78-79:118-122. doi:10.1016/j.jpba.2013.01.043
184. Myhr G, Moan J. Synergistic and tumour selective effects of chemotherapy and ultrasound treatment. *Cancer Lett*. 2006;232(2):206-213. doi:10.1016/j.canlet.2005.02.020
185. Evjen TJ, Hagtvet E, Nilssen EA, Brandl M, Fossheim SL. Sonosensitive dioleoylphosphatidylethanolamine-containing liposomes with prolonged blood circulation time of doxorubicin. *Eur J Pharm Sci*. 2011;43(4):318-324. doi:10.1016/j.ejps.2011.05.007
186. Javadi M, Pitt WG, Tracy CM, et al. Ultrasonic gene and drug delivery using eLiposomes. *J Control Release*. 2013;167(1):92-100. doi:10.1016/j.jconrel.2013.01.009
187. Hussein GA, Pitt WG, Williams JB, Javadi M. Investigating the Release Mechanism of Calcein from eLiposomes at Higher Temperatures. *J Colloid Sci Biotechnol*. 2015;3(3):239-244. doi:10.1166/jcsb.2014.1100
188. Fan X, Wang L, Guo Y, Xiong X, Zhu L, Fang K. Inhibition of prostate cancer growth using doxorubicin assisted by ultrasound-targeted nanobubble destruction. *Int J*

- Nanomedicine*. 2016;Volume 11:3585-3596. doi:10.2147/IJN.S111808
189. Ueno Y, Sonoda S, Suzuki R, et al. Combination of ultrasound and bubble liposome enhance the effect of doxorubicin and inhibit murine osteosarcoma growth. *Cancer Biol Ther*. 2011;12(4):270-277. doi:10.4161/cbt.12.4.16259
190. Lyon PC, Griffiths LF, Lee J, et al. Clinical trial protocol for TARDOX: A phase I study to investigate the feasibility of targeted release of lyso-thermosensitive liposomal doxorubicin (ThermoDox®) using focused ultrasound in patients with liver tumours. *J Ther Ultrasound*. 2017;5(1). doi:10.1186/s40349-017-0104-0
191. Van Ballegoie C, Man A, Win M, Yapp DT. Spatially specific liposomal cancer therapy triggered by clinical external sources of energy. *Pharmaceutics*. 2019;11(3). doi:10.3390/pharmaceutics11030125
192. Boissenot T, Bordat A, Fattal E, Tsapis N. Ultrasound-triggered drug delivery for cancer treatment using drug delivery systems: From theoretical considerations to practical applications. *J Control Release*. 2016;241:144-163. doi:10.1016/j.jconrel.2016.09.026
193. Farr N, Wang YN, D'Andrea S, et al. Hyperthermia-enhanced targeted drug delivery using magnetic resonance-guided focussed ultrasound: a pre-clinical study in a genetic model of pancreatic cancer. *Int J Hyperth*. 2018;34(3):284-291. doi:10.1080/02656736.2017.1336675
194. Zagar TM, Vujaskovic Z, Formenti S, et al. Two phase I dose-escalation/pharmacokinetics studies of low temperature liposomal doxorubicin (LTLD) and mild local hyperthermia in heavily pretreated patients with local regionally recurrent breast cancer. *Int J Hyperth*. 2014;30(5):285-294. doi:10.3109/02656736.2014.936049
195. Gray MD, Lyon PC, Mannaris C, et al. Focused ultrasound hyperthermia for targeted drug release from thermosensitive liposomes: Results from a phase I trial. *Radiology*. 2019;291(1):232-238. doi:10.1148/radiol.2018181445
196. Rizzitelli S, Giustetto P, Cutrin JC, et al. Sonosensitive theranostic liposomes for preclinical in vivo MRI-guided visualization of doxorubicin release stimulated by pulsed low intensity non-focused ultrasound. *J Control Release*. 2015;202:21-30. doi:10.1016/j.jconrel.2015.01.028
197. Dromi S, Frenkel V, Luk A, et al. Pulsed-high intensity focused ultrasound and low temperature - Sensitive liposomes for enhanced targeted drug delivery and antitumor effect. *Clin Cancer Res*. 2007;13(9):2722-2727. doi:10.1158/1078-0432.CCR-06-2443
198. Kheirloom A, Lai CY, Tam SM, et al. Complete regression of local cancer using temperature-sensitive liposomes combined with ultrasound-mediated hyperthermia. *J Control Release*. 2013;172(1):266-273. doi:10.1016/j.jconrel.2013.08.019
199. Lattin JR, Pitt WG, Belnap DM, Hussein GA. Ultrasound-Induced Calcein Release From eLiposomes. *Ultrasound Med Biol*. 2012;38(12):2163-2173. doi:10.1016/j.ultrasmedbio.2012.08.001
200. Um W, Kwon S, You DG, Cha JM, Kim HR, Park JH. Non-thermal acoustic treatment as a safe alternative to thermosensitive liposome-involved hyperthermia for cancer therapy. *RSC Adv*. 2017;7(47):29618-29625. doi:10.1039/c7ra02065a
201. Santos MA, Goertz DE, Hynynen K. Focused ultrasound hyperthermia mediated drug delivery using thermosensitive liposomes and visualized with in vivo two-photon microscopy. *Theranostics*. 2017;7(10):2718-2731. doi:10.7150/thno.19662
202. Awad NS, Paul V, Al-Sayah MH, Hussein GA. Ultrasonically controlled albumin-conjugated liposomes for breast cancer therapy. *Artif Cells, Nanomedicine, Biotechnol*. 2019;47(1):705-714. doi:10.1080/21691401.2019.1573175
203. Lentacker I, Geers B, Demeester J, De Smedt SC, Sanders NN. Design and Evaluation of Doxorubicin-containing Microbubbles for Ultrasound-triggered Doxorubicin Delivery: Cytotoxicity and Mechanisms Involved. *Mol Ther*. 2010;18(1):101-108. doi:10.1038/mt.2009.160
204. Yang F-Y, Wong T-T, Teng M-C, et al. Focused ultrasound and interleukin-4 receptor-targeted liposomal doxorubicin for enhanced targeted drug delivery and antitumor effect in glioblastoma multiforme. *J Control Release*. 2012;160(3):652-658. doi:10.1016/j.jconrel.2012.02.023
205. Novell A, Al Sabbagh C, Escoffre J-M, et al. Focused ultrasound influence on calcein-loaded thermosensitive stealth liposomes. *Int J Hyperth*. 2015;31(4):349-358. doi:10.3109/02656736.2014.1000393
206. Treat LH, McDannold N, Zhang Y, Vykhodtseva N, Hynynen K. Improved Anti-Tumor Effect of Liposomal Doxorubicin After Targeted Blood-Brain Barrier Disruption by MRI-Guided Focused Ultrasound in Rat Glioma. *Ultrasound Med Biol*. 2012;38(10):1716-1725. doi:10.1016/j.ultrasmedbio.2012.04.015
207. Park SM, Kim MS, Park S-J, et al. Novel temperature-triggered liposome with high stability: Formulation, in vitro evaluation, and in vivo study combined with high-intensity focused ultrasound (HIFU). *J Control Release*. 2013;170(3):373-379. doi:10.1016/j.jconrel.2013.06.003
208. Pitt WG, Hussein GA, Roeder BL, et al. Preliminary results of combining low frequency low intensity ultrasound and liposomal drug delivery to treat tumors in rats. *J Nanosci Nanotechnol*. 2011;11(3):1866-1870. doi:10.1166/jnn.2011.3117
209. Eggen S, Afadzi M, Nilssen EA, Haugstad SB, Angelsen B, Davies C de L. Ultrasound mediated delivery of liposomal doxorubicin in prostate tumor tissue. *2012 IEEE Int Ultrason Symp*. 2012. doi:10.1109/ultsym.2012.0108
210. Ranjan A, Jacobs GC, Woods DL, et al. Image-guided drug delivery with magnetic resonance guided high intensity focused ultrasound and temperature sensitive liposomes in a rabbit Vx2 tumor model. *J Control Release*. 2012;158(3):487-494. doi:10.1016/j.jconrel.2011.12.011
211. Salkho NM, Paul V, Kawak P, et al. Ultrasonically controlled estrone-modified liposomes for estrogen-positive breast cancer therapy. *Artif Cells, Nanomedicine, Biotechnol*. 2018;46(sup2):462-472. doi:10.1080/21691401.2018.1459634
212. Aryal M, Vykhodtseva N, Zhang YZ, Park J, McDannold N. Multiple treatments with liposomal doxorubicin and ultrasound-induced disruption of blood-tumor and blood-brain barriers improve outcomes in a rat glioma model. *J Control Release*. 2013;169(1-2):103-111. doi:10.1016/j.jconrel.2013.04.007
213. Williams JB, Buchanan CM, Pitt WG. Codelivery of

- Doxorubicin and Verapamil for Treating Multidrug Resistant Cancer Cells. *Pharm Nanotechnol.* 2018;6(2):116-123. doi:10.2174/2211738506666180316122620
214. Centelles MN, Wright M, So P-W, et al. Image-guided thermosensitive liposomes for focused ultrasound drug delivery: Using NIRF-labelled lipids and topotecan to visualise the effects of hyperthermia in tumours. *J Control Release.* 2018;280:87-98. doi:10.1016/j.jconrel.2018.04.047
215. Lin C-Y, Javadi M, Belnap DM, Barrow JR, Pitt WG. Ultrasound sensitive eLiposomes containing doxorubicin for drug targeting therapy. *Nanomedicine Nanotechnology, Biol Med.* 2014;10(1):67-76. doi:10.1016/j.nano.2013.06.011
216. Hamano N, Negishi Y, Omata D, et al. Bubble Liposomes and Ultrasound Enhance the Antitumor Effects of AG73 Liposomes Encapsulating Antitumor Agents. *Mol Pharm.* 2013;10(2):774-779. doi:10.1021/mp300463h
217. Awad NS, Paul V, Mahmoud MS, et al. Effect of Pegylation and Targeting Moieties on the Ultrasound-Mediated Drug Release from Liposomes. *ACS Biomater Sci Eng.* 2020;6(1):48-57. doi:10.1021/acsbomaterials.8b01301
218. Unger EC, Porter T, Culp W, Labell R, Matsunaga T, Zutshi R. Therapeutic applications of lipid-coated microbubbles. *Adv Drug Deliv Rev.* 2004;56(9):1291-1314. doi:10.1016/j.addr.2003.12.006
219. Huang C, Zhang H, Bai R. Advances in ultrasound-targeted microbubble-mediated gene therapy for liver fibrosis. *Acta Pharm Sin B.* 2017;7(4):447-452. doi:10.1016/j.apsb.2017.02.004
220. Ferrara K, Pollard R, Borden M. Ultrasound Microbubble Contrast Agents: Fundamentals and Application to Gene and Drug Delivery. *Annu Rev Biomed Eng.* 2007;9(1):415-447. doi:10.1146/annurev.bioeng.8.061505.095852
221. Bekeredjian R, Chen S, Grayburn PA, Shohet R V. Augmentation of cardiac protein delivery using ultrasound targeted microbubble destruction. *Ultrasound Med Biol.* 2005;31(5):687-691. doi:10.1016/j.ultrasmedbio.2004.08.002
222. Shamout FE, Pouliopoulos AN, Lee P, et al. Enhancement of Non-Invasive Trans-Membrane Drug Delivery Using Ultrasound and Microbubbles During Physiologically Relevant Flow. *Ultrasound Med Biol.* 2015;41(9):2435-2448. doi:10.1016/j.ultrasmedbio.2015.05.003
223. Geers B, Lentacker I, Sanders NN, Demeester J, Meairs S, De Smedt SC. Self-assembled liposome-loaded microbubbles: The missing link for safe and efficient ultrasound triggered drug-delivery. *J Control Release.* 2011;152(2):249-256. doi:10.1016/j.jconrel.2011.02.024
224. Escoffre J, Mannaris C, Geers B, et al. Doxorubicin liposome-loaded microbubbles for contrast imaging and ultrasound-triggered drug delivery. *IEEE Trans Ultrason Ferroelectr Freq Control.* 2013;60(1). doi:10.1109/tuffc.2013.2539
225. Kheirloomoom A, Dayton PA, Lum AFH, et al. Acoustically-active microbubbles conjugated to liposomes: Characterization of a proposed drug delivery vehicle. *J Control Release.* 2007;118(3):275-284. doi:10.1016/j.jconrel.2006.12.015
226. Böhmer MR, Chlon CHT, Raju BI, Chin CT, Shevchenko T, Klibanov AL. Focused ultrasound and microbubbles for enhanced extravasation. *J Control Release.* 2010;148(1):18-24. doi:10.1016/j.jconrel.2010.06.012
227. Zhang J, Wang S, Deng Z, et al. Ultrasound-Triggered Drug Delivery for Breast Tumor Therapy Through iRGD-Targeted Paclitaxel-Loaded Liposome-Microbubble Complexes. *J Biomed Nanotechnol.* 2018;14(8):1384-1395. doi:10.1166/jbn.2018.2594
228. Yan F, Li L, Deng Z, et al. Paclitaxel-liposome-microbubble complexes as ultrasound-triggered therapeutic drug delivery carriers. *J Control Release.* 2013;166(3):246-255. doi:10.1016/j.jconrel.2012.12.025
229. Yu FTH, Chen X, Wang J, Qin B, Villanueva FS. Low Intensity Ultrasound Mediated Liposomal Doxorubicin Delivery Using Polymer Microbubbles. *Mol Pharm.* 2016;13(1):55-64. doi:10.1021/acs.molpharmaceut.5b00421
230. Majidinia M, Mirza-Aghazadeh-Attari M, Rahimi M, et al. Overcoming multidrug resistance in cancer: Recent progress in nanotechnology and new horizons. *IUBMB Life.* 2020;72(5):855-871. doi:10.1002/iub.2215
231. Das M, Musetti S, Huang L. RNA Interference-Based Cancer Drugs: The Roadblocks, and the "Delivery" of the Promise. *Nucleic Acid Ther.* 2019;29(2):61-66. doi:10.1089/nat.2018.0762
232. Krishna R, Mayer LD. Multidrug resistance (MDR) in cancer: Mechanisms, reversal using modulators of MDR and the role of MDR modulators in influencing the pharmacokinetics of anticancer drugs. *Eur J Pharm Sci.* 2000;11(4):265-283. doi:10.1016/S0928-0987(00)00114-7
233. Zuckerman JE, Davis ME. Clinical experiences with systemically administered siRNA-based therapeutics in cancer. *Nat Rev Drug Discov.* 2015;14(12):843-856. doi:10.1038/nrd4685
234. Barata P, Sood AK, Hong DS. RNA-targeted therapeutics in cancer clinical trials: Current status and future directions. *Cancer Treat Rev.* 2016;50:35-47. doi:10.1016/j.ctrv.2016.08.004
235. Afadzi M, Davies C de L, Hansen YH, et al. Effect of Ultrasound Parameters on the Release of Liposomal Calcein. *Ultrasound Med Biol.* 2012;38(3):476-486. doi:10.1016/j.ultrasmedbio.2011.11.017
236. Schroeder A, Avnir Y, Weisman S, et al. Controlling Liposomal Drug Release with Low Frequency Ultrasound: Mechanism and Feasibility. *Langmuir.* 2007;23(7):4019-4025. doi:10.1021/LA0631668
237. Pong M, Umchid S, Guarino AJ, et al. In vitro ultrasound-mediated leakage from phospholipid vesicles. *Ultrasonics.* 2006;45(1-4):133-145. doi:10.1016/j.ultras.2006.07.021
238. Hussein GA, Diaz de la Rosa MA, Richardson ES, Christensen DA, Pitt WG. The role of cavitation in acoustically activated drug delivery. *J Control Release.* 2005;107(2):253-261. doi:10.1016/j.jconrel.2005.06.015
239. Gonciar D, Mocan T, Matea CT, et al. Nanotechnology in metastatic cancer treatment: Current achievements and future research trends. *J Cancer.* 2019;10(6):1358-1369. doi:10.7150/jca.28394
240. Zhang W, Wang F, Hu C, Zhou Y, Gao H, Hu J. The progress and perspective of nanoparticle-enabled tumor metastasis treatment. *Acta Pharm Sin B.* July 2020. doi:10.1016/j.apsb.2020.07.013
241. Rosenblum D, Joshi N, Tao W, Karp JM, Peer D. Progress and challenges towards targeted delivery of cancer

- therapeutics. *Nat Commun.* 2018;9(1). doi:10.1038/s41467-018-03705-y
242. Yang L, Shi P, Zhao G, et al. Targeting cancer stem cell pathways for cancer therapy. *Signal Transduct Target Ther.* 2020;5(1):1-35. doi:10.1038/s41392-020-0110-5
243. Bao B, Ahmad A, Azmi AS, Ali S, Sarkar FH. Overview of cancer stem cells (CSCs) and mechanisms of their regulation: Implications for cancer therapy. *Curr Protoc Pharmacol.* 2013;Chapter 14(SUPPL.61). doi:10.1002/0471141755.ph1425s61
244. Plaks V, Kong N, Werb Z. The cancer stem cell niche: How essential is the niche in regulating stemness of tumor cells? *Cell Stem Cell.* 2015;16(3):225-238. doi:10.1016/j.stem.2015.02.015
245. Jin J, Bhujwalla ZM. Biomimetic Nanoparticles Camouflaged in Cancer Cell Membranes and Their Applications in Cancer Theranostics. *Front Oncol.* 2020;9:1560. doi:10.3389/fonc.2019.01560
246. Li A, Zhao J, Fu J, Cai J, Zhang P. Recent advances of biomimetic nano-systems in the diagnosis and treatment of tumor. *Asian J Pharm Sci.* September 2019. doi:10.1016/j.ajps.2019.08.001
247. Peinado H, Zhang H, Matei IR, et al. Pre-metastatic niches: Organ-specific homes for metastases. *Nat Rev Cancer.* 2017;17(5):302-317. doi:10.1038/nrc.2017.6
248. Huang W, Chen L, Kang L, et al. Nanomedicine-based combination anticancer therapy between nucleic acids and small-molecular drugs. *Adv Drug Deliv Rev.* 2017;115:82-97. doi:10.1016/j.addr.2017.06.004
249. Krzyszczyk P, Acevedo A, Davidoff EJ, et al. The growing role of precision and personalized medicine for cancer treatment. *TECHNOLOGY.* 2018;06(03n04):79-100. doi:10.1142/s2339547818300020
250. Malone ER, Oliva M, Sabatini PJB, Stockley TL, Siu LL. Molecular profiling for precision cancer therapies. *Genome Med.* 2020;12(1):8. doi:10.1186/s13073-019-0703-1
251. Le Tourneau C, Borcoman E, Kamal M. Molecular profiling in precision medicine oncology. *Nat Med.* 2019;25(5):711-712. doi:10.1038/s41591-019-0442-2
252. Bartelink IH, Jones EF, Shahidi-Latham SK, et al. Tumor Drug Penetration Measurements Could Be the Neglected Piece of the Personalized Cancer Treatment Puzzle. *Clin Pharmacol Ther.* 2019;106(1):148-163. doi:10.1002/cpt.1211
253. Torchilin VP. Targeted pharmaceutical nanocarriers for cancer therapy and imaging. *AAPS J.* 2007;9(2):E128-E147. doi:10.1208/aapsj0902015
254. Ventola CL. Progress in nanomedicine: Approved and investigational nanodrugs. *P T.* 2017;42(12):742-755. /pmc/articles/PMC5720487/?report=abstract. Accessed September 9, 2020.
255. Grossman JH, Crist RM, Clogston JD. Early Development Challenges for Drug Products Containing Nanomaterials. *AAPS J.* 2016;19(1):92-102. doi:10.1208/s12248-016-9980-4
256. Elsaesser A, Howard CV. Toxicology of nanoparticles. *Adv Drug Deliv Rev.* 2012;64(2):129-137. doi:10.1016/j.addr.2011.09.001
257. Pan Y, Neuss S, Leifert A, et al. Size-Dependent Cytotoxicity of Gold Nanoparticles. *Small.* 2007;3(11):1941-1949. doi:10.1002/smll.200700378
258. Zhang B, Sai Lung P, Zhao S, Chu Z, Chrzanowski W, Li Q. Shape dependent cytotoxicity of PLGA-PEG nanoparticles on human cells. *Sci Rep.* 2017;7(1). doi:10.1038/s41598-017-07588-9
259. Kermanizadeh A, Jacobsen NR, Roursgaard M, Loft S, Møller P. Hepatic toxicity assessment of cationic liposome exposure in healthy and chronic alcohol fed mice. *Heliyon.* 2017;3(11):e00458. doi:10.1016/j.heliyon.2017.e00458
260. Borm PJA, Robbins D, Haubold S, et al. The potential risks of nanomaterials: A review carried out for ECETOC. *Part Fibre Toxicol.* 2006;3. doi:10.1186/1743-8977-3-11